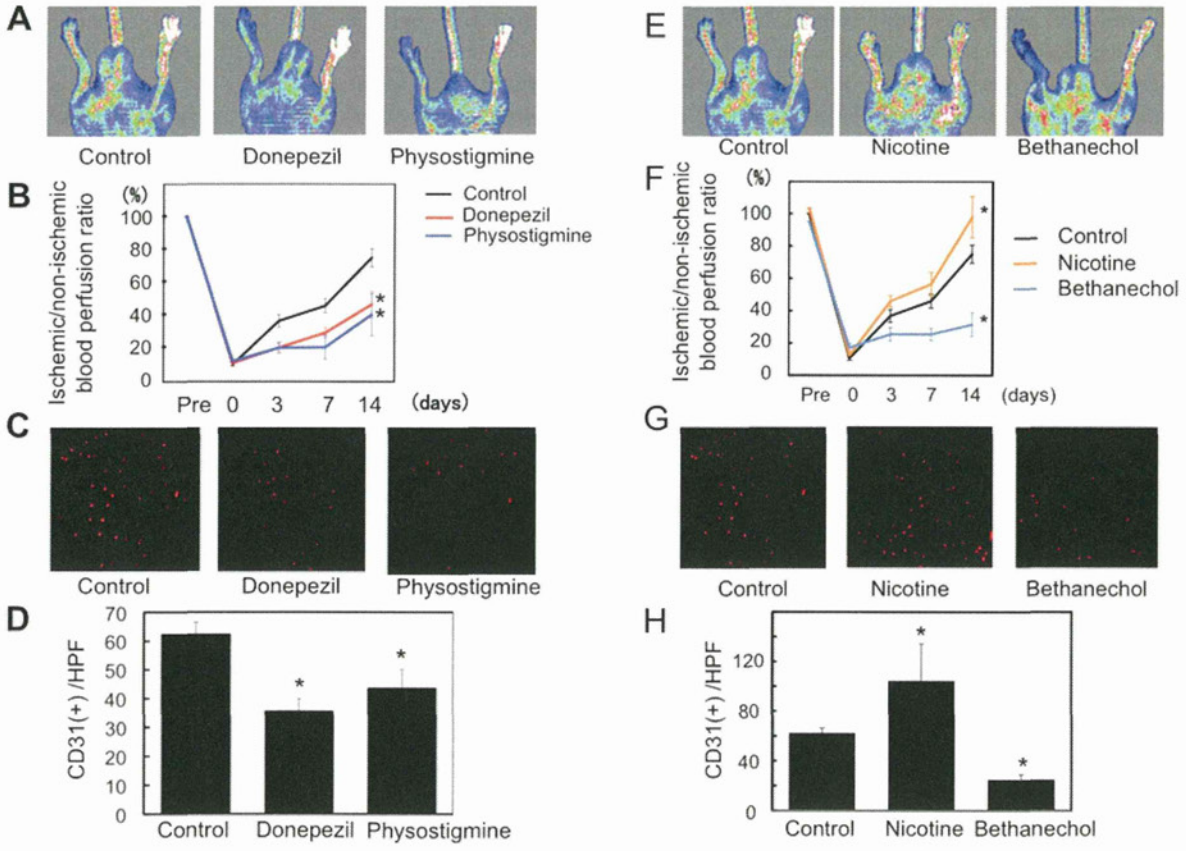

Figure 1 Acetylcholinesterase inhibitors attenuate neovascularization in a mouse model of hindlimb ischaemia

The effect of donepezil or physostigmine on blood flow recovery after hindlimb ischaemia was examined (A–D). The effect of bethanechol or nicotine on blood flow recovery after hindlimb ischaemia was examined (E–H). (A, E), Representative laser Doppler perfusion images of blood flow after 2 weeks of hindlimb ischaemia are shown. (B, F) Ratio of blood flow in the ischaemic hindlimb to that in the non-ischaemic hindlimb measured immediately (day 0) and at the days indicated in the Figure after unilateral femoral artery ligation. (C, G) Immunohistochemical staining for CD31 in the gastrocnemial muscle of ischaemic hindlimb is shown. (D, H) Capillary density expressed as the number of capillaries per HPF (high-power field). Results are expressed as means $\pm$ S.E.M. ($n = 7$). $^*P < 0.05$ compared with the control group.

nAChR (nicotinic ACh receptor; nicotine) on the blood flow recovery and capillary density of the ischaemic hindlimb (Figures 1E–1H). Bethanechol reduced blood flow recovery and capillary density of the ischaemic hindlimb, suggesting that mAChR is responsible for the attenuation of blood flow recovery by cholinergic stimulation. In contrast, nicotine enhanced blood flow recovery. Although the mechanism is not clear, the net effect of acetylcholinesterase inhibitors on angiogenesis favours mAChR stimulation in our model.

Donepezil suppressed VEGF and IL-1β expression in the ischaemic hindlimb

mRNA expression of angiogenic factors and cytokines in the ischaemic hindlimb harvested at day 7 was examined (Figure 2A). The expression of VEGF mRNA was significantly decreased in the donepezil-treated mice. However, expression of other angiogenic factors including bFGF, PDGF, PLGF (placental growth factor), Angpt (angiopoietin) 1 and 2 was not affected by donepezil treatment. Expression of IL-1β and TNFα mRNA in the ischaemic hindlimb was significantly decreased in the donepezil-treated group, suggesting an anti-inflammatory effect of donepezil. qRT–PCR also showed a trend towards reduction of CD3ε (T-lymphocytes) and F4/80 (macrophages) mRNA in the ischaemic hindlimb of the donepezil-treated mice compared with that of control mice. Although the difference was not statistically significant, the results suggest that treatment with donepezil mildly suppressed infiltration of inflammatory cells into the ischaemic hindlimb.

Protein level of IL-1β was significantly suppressed in an ischaemic hindlimb of donepezil-treated mice (Figure 2B). Although VEGF level was also decreased in an ischaemic hindlimb of donepezil-treated mice, the difference of VEGF level between control and donepezil-treated mice showed a borderline significance. We could not detect any changes in the serum levels of IL-1β, IL-6,

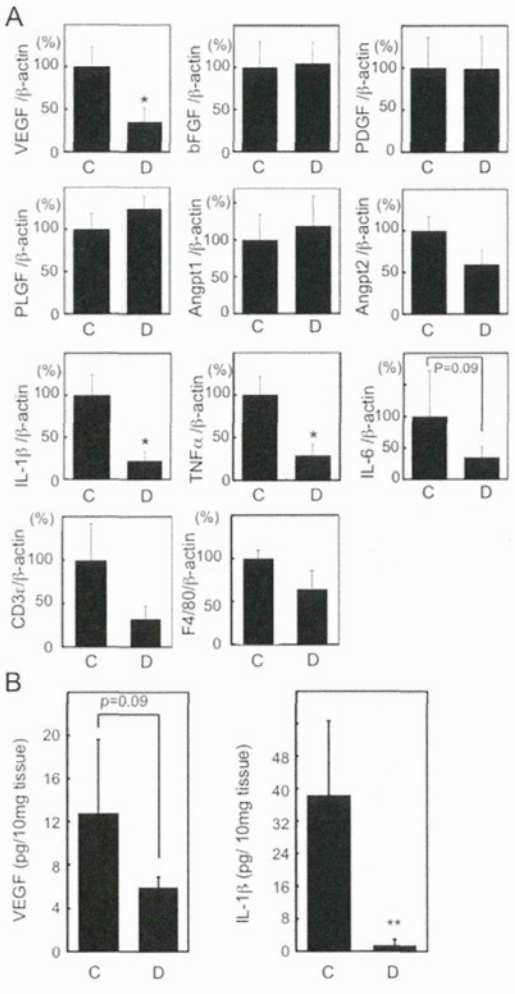

Figure 2 mRNA and protein expression in the ischaemic hindlimb of control and donepezil-treated mice

(A) mRNA expression of angiogenic factors and inflammatory cytokines in the ischaemic hindlimb of control (bar C) and donepezil-treated (bar D) mice was quantified with real time RT–PCR. The primer sequences used are indicated in Supplementary Table S1 at http://www.clinsci.org/cs/123/cs1230241add.htm. The expression level of each mRNA in the ischaemic hindlimb of control mouse was set as 100% ($n = 7$). $^*P < 0.05$ compared with the control group. (B) Protein level of IL-1β and VEGF in the ischaemic hindlimb of control and donepezil-treated mice was measured by ELISA ($n = 4$). $^*P < 0.05$ compared with the control group.

or VEGF (results not shown). TNFα was not detectable in the serum and in ischaemic hindlimb in both groups. These findings suggest that donepezil locally suppressed inflammation in an ischaemic hindlimb.

IL-1β reversed the anti-angiogenic effect of donepezil

A previous report showed that recipient-derived IL-1β plays an important role in blood flow recovery in the ischaemic hindlimb [10,17]. As IL-1β expression was decreased in the ischaemic hindlimb of the donepezil-treated mice, we injected recombinant murine IL-1β into the ischaemic hindlimb. An injection of IL-1β restored the reduced blood flow recovery (Figures 3A and 3B) and capillary formation (Figures 3C and 3D) in the donepezil-treated mice. Donepezil-induced suppression of VEGF mRNA expression in the ischaemic hindlimb was also reversed by the IL-1β injection (Figure 3E). The IL-1β injection did not cause haemodynamic changes (see Supplementary Table S3 at http://www.clinsci.org/cs/123/cs1230241add.htm).

Role of PI3K (phosphoinositide 3-kinase) pathway in hypoxia-induced IL-1β induction

To gain an insight into the mechanism of donepezil inhibition of IL-1β expression, we used C2C12 cells, a mouse embryonic myoblast cell line. As hindlimb muscles are exposed to hypoxic conditions after femoral artery ligation, the effect of low oxygen concentration (1% O_2) on IL-1β mRNA expression was determined. After exposure to the hypoxic condition for 12 h, IL-1β mRNA level was significantly increased compared with that in C2C12 cells incubated in normoxic (20% O_2) conditions (Figure 4A). The induction of IL-1β by hypoxic conditions was significantly inhibited by pre-incubation with ACh. The Ach-induced suppression of IL-1β was reversed by the presence of atropine, a competitive antagonist of mAChR, but not by mecamylamine, a specific antagonist of nAChR. These results indicate that mAChR is responsible for the suppression of hypoxia-induced IL-1β expression. The findings are consistent with the *in vivo* results that a mAChR agonist bethanechol inhibited angiogenesis.

It was reported that PI3K and MAPKs are involved in IL-1β induction [18]. Treatment with LY294002 (PI3K inhibitor), PD98059 (ERK kinase inhibitor) or SP600125 (JNK inhibitor) significantly decreased hypoxia-induced IL-1β mRNA expression (Figure 4B). ACh attenuated hypoxia-induced phosphorylation of Akt, a downstream kinase of PI3K, but did not affect phosphorylation of ERK, JNK or p38 MAPK in C2C12 cells (Figures 4C–4F). These results suggest that ACh may suppress hypoxia-induced IL-1β expression through inhibition of the PI3K/Akt pathway. Indeed, the phosphorylation level of Akt but not other MAPKs was decreased in the ischaemic hindlimb of donepezil-treated mice (Figures 4G–4J).

DISCUSSION

We have shown in the present study that treatment with donepezil attenuated blood flow recovery of the ischaemic hindlimb in mice through reduction of the expression of IL-1β. It was suggested that mAChR is involved in this process. ACh as well as PI3K inhibitor suppressed hypoxia-induced IL-1β induction

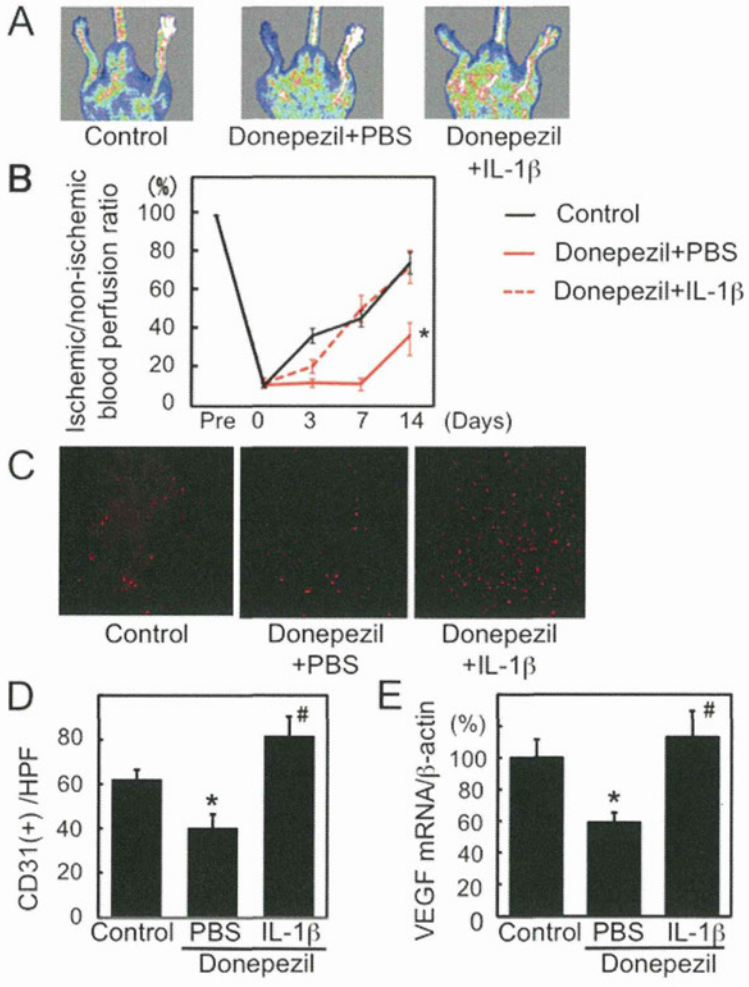

Figure 3 IL-1β reverses donepezil-induced inhibition of neovascularization

(A) Representative laser Doppler perfusion images of blood flow in the ischaemic hindlimb of donepezil-treated mice with or without IL-1β injection are shown. Control indicates ischaemic hindlimb without donepezil treatment. (B) Ratio of blood flow in the ischaemic hindlimb to that in the non-ischaemic hindlimb. $^{*}P < 0.05$ compared with control. (C) Immunohistochemical staining for CD31 in the gastrocnemial muscle of ischaemic hindlimb is shown. (D) Capillary density that is expressed as the number of capillaries per HPF. (E) mRNA expression of VEGF was quantified with real-time RT–PCR. Results are expressed as means $\pm$ S.E.M. ($n = 6-8$). $^{*}P < 0.05$ compared with control; $^{\#}P < 0.05$ compared with donepezil + PBS.

in C2C12 cells. Donepezil suppressed Akt activation in the ischaemic hindlimb, suggesting that an increase in Ach level by donepezil may inhibit hypoxia-induced IL-1β induction through suppression of the PI3K/Akt pathway, resulting in the inhibition of VEGF induction and angiogenesis.

A recent meta-analysis by Singh et al. [19] revealed that inhalation of anti-cholinergics is associated with a significant increase in the risk of cardiovascular events in patients with COPD (chronic obstructive pulmonary disease). Inhalation of anti-cholinergics significantly increased the risk of myocardial infarction and cardiovascular death without a statistically significant effect on the risk of stroke. This meta-analysis may support the idea that anti-cholinergics, contrary to acetylcholinesterase inhibitors, accelerate angiogenesis in the atherosclerotic plaque and thereby increase its vulnerability, which results in an increase in the cardiovascular events. However, a very recent double-blind trial that examined the effect of tiotropium, one of the anti-cholinergics, in patients with COPD showed opposite results [20]. Treatment with tiotropium showed an insignificant decrease in the number of death in patients with COPD and significantly decreased the incidence of myocardial infarction compared with placebo. Therefore the issue regarding the effect of anti-cholinergics treatment on cardiovascular events is still controversial.

Stimulation of nAChR is reported to enhance proliferation of endothelial cells and angiogenesis [13], which is consistent with the present study. Although stimulation of mAChR by bethanechol suppressed angiogenesis, the mechanism by which acetylcholinesterase inhibitors that

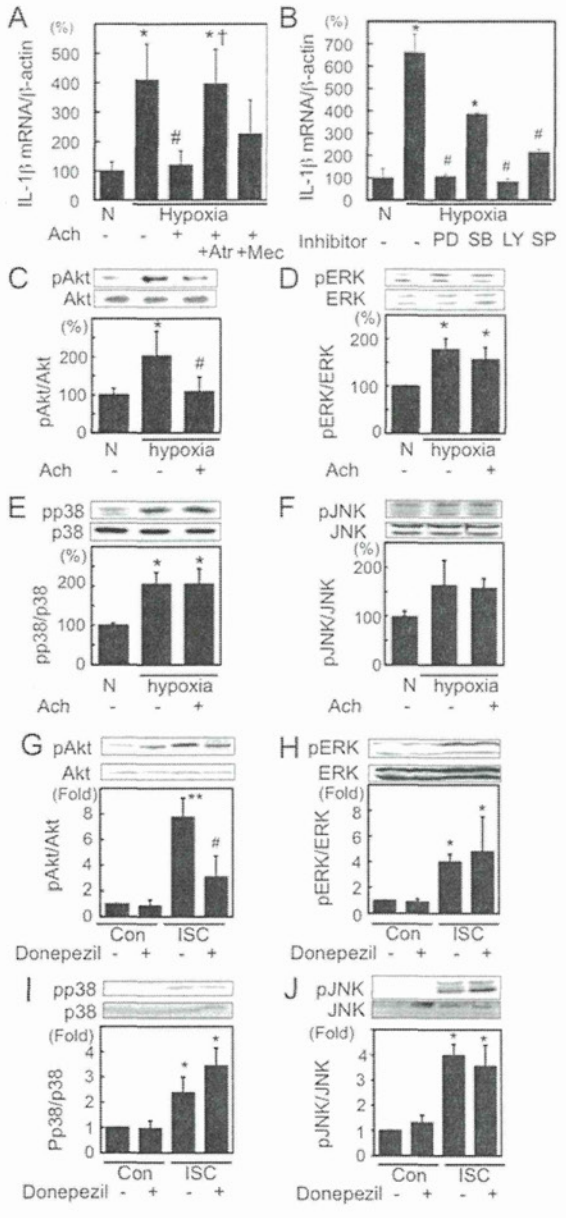

Figure 4 **Ach and donepezil suppresses Akt activation**

(A) C2C12 myoblast cells were pre-incubated with ACh (100 nmol/l) in the presence of atropine (Atr, 10 μmol/l) or mecamylamine (Mec, 10 μmol/l) prior to exposure to hypoxia (1 % O_2) for 1 h. After exposure to hypoxic condition for 12 h, the IL-1β mRNA level was determined with real time RT–PCR. N, normoxia. (B) The effects of PD98059 (PD; an ERK inhibitor, 10 μmol/l), SB203580 (SB; a p38 MAPK inhibitor, 10 μmol/l), LY294002 (LY; a PI3K inhibitor, 10 μmol/l) and SP600125 (SP; a JNK inhibitor, 10 μmol/l) on hypoxia-induced IL-1β mRNA expression in C2C12 cells were examined. mRNA expression of IL-1β in C2C12 cells cultured under normoxia (N) is used as control. $^{*}P < 0.05$ compared with under normoxic conditions; $^{\#}P < 0.05$ compared with hypoxia; $^{\dagger}P < 0.05$ compared with hypoxia + Ach ($n = 4$). (C–F) Effect of ACh on hypoxia-induced activation of Akt and MAPK was examined. (G–J) Effect of donepezil on the activation of Akt and MAPK in the non-ischaemic (Con) and ischaemic (ISC) hindlimb was examined. The ratio of phosphorylated form to total protein level of each kinase is shown in the histograms ($n = 4$). $^{*}P < 0.05$ compared with control, $^{\#}P < 0.05$ compared with the ischaemic hindlimb without donepezil.

are supposed to stimulate both nAChR and mAChR mimic the effect of mAChR is not clear.

Our *in vitro* results suggest that the increased ACh may be targeting ischaemic muscle of hindlimb, because Ach inhibited hypoxia-induced IL-1β expression in myoblast cells and donepezil reduced IL-1β expression in the ischaemic hindlimb. Therefore the anti-inflammatory effect of ACh on regenerating skeletal muscle may be dominant compared with direct effects of Ach on endothelial cells. Although we cannot exclude possible non-specific effects of these acetylcholinesterase inhibitors on angiogenesis, this is unlikely because the structure of donepezil and physostigmine is quite different.

The source of ACh in this hindlimb ischaemia model is not clear at this point. It is possible that an increase in ACh in the motor nerve ending of neuromuscular junction may play a role. Recent studies suggest that macrophages express choline acetyltransferase, which produces Ach from choline and acetyl-CoA [21]. Therefore infiltrated inflammatory cells may be another possible source of ACh. Alternatively, the ischaemic muscle itself may be the source of ACh, because it was previously reported that immunoreactivity of choline acetyltransferase is observed in both myoblasts and myotubes [22]. Another possibility is that acetylcholinesterase inhibitors may suppress angiogenesis in an indirect manner. mAChR in the CNS is reported to be involved in cholinergic anti-inflammatory pathway. Intracerebroventricular administration of muscarine, an agonist for mAChR, inhibited LPS-induced production of TNFα in the serum [23]. We cannot exclude the possible effect of these acetylcholinesterase inhibitors on the CNS in mediating an anti-angiogenic effect. Further study is needed to clarify the source and target cells of ACh in the ischaemic hindlimb.

A recent report showed that chronic hypoxia increased Akt phosphorylation in human macrophages [24]. Another report showed that TNFα-induced IL-1β expression is dependent on PI3K/Akt and NF-κB activation [18]. We showed that Ach suppressed hypoxia-induced IL-1β expression and Akt phosphorylation in C2C12 cells. And PI3K inhibitor suppressed hypoxia-induced IL-1β expression. Therefore it is suggested that Ach suppresses hypoxia-induced IL-1β expression through inhibition of PI3K/Akt pathway. Although it is known that PTEN (phosphatase and tensin homologue deleted on chromosome 10) negatively regulates PI3K/Akt pathway, we could not detect any change in PTEN expression in the ischaemic hindlimb in donepezil-treated mice (results not shown). The mechanism by which Ach inhibition of hypoxia-induced PI3K/Akt pathway is not clear and further study is needed.

The limitation of the present study is that the dose of donepezil used in this study is very high compared with

that clinically used for treatment of patients with AD. Therefore we must be cautious whether donepezil at a clinical dose affects angiogenesis in patients. A dose of 5–10 mg/kg of body weight per day of donepezil used in this study is widely used to examine the effect of donepezil on dementia in a rodent model [12] despite the fact that the clinical dose is 5–10 mg/day for patients with AD. It may be possible that differential susceptibility to the drug between humans and mice account for the requirement for high dose of donepezil in rodent models. A recent study showed a very small increase in skin temperature in the ischaemic hindlimb by donepezil, suggesting an angiogenic effect of donepezil [25]. The reason for the discrepancy between the previous study and our study is not clear at this point. However, the dose of donepezil administered to mice is higher in this study compared with the previous study (5 mg/kg of body weight per day), which may explain the discrepancy. Alternatively, the discrepancy may be because the previous report measured skin temperature rather than blood flow. In addition, the authors failed to examine the time course and measured surface temperature at later stage (28 days after ligation of femoral artery). We could not exclude the possibility that the difference of blood flow recovery of ischaemic hindlimb between control and donepezil-treated mice disappears or reverses after day 14 of femoral artery ligation. However, most of the study using C57BL/6 mice showed that blood flow recovery after hindlimb ischaemia reaches a plateau at day 14 or 21 [26,27]. Therefore this possibility is unlikely. And an anti-angiogenic effect of acetylcholinesterase inhibitor is confirmed by physostigmine in our study. Therefore it is suggested that acetylcholinesterase inhibitor has an anti-angiogenic effect at least under our experimental conditions.

In summary, we have shown in the present study that treatment with donepezil attenuated angiogenesis. Stimulation of cholinergic system may be a novel anti-angiogenic therapy.

AUTHOR CONTRIBUTION

Ryohei Miyazaki, Toshihiro Ichiki, Kotaro Takeda and Kenji Sunagawa contributed to the conception and design of the study, and writing of the paper. Ryohei Miyazaki performed the experiments. Jiro Ikeda, Aya Kamiharaguchi, Toru Hashimoto, Eriko Narabayashi and Hirohide Matsuura contributed to the *in vivo* experiments.

ACKNOWLEDGEMENT

We thank the Research Support Center, Kyushu University Graduate School of Medical Sciences for technical support.

FUNDING

This study was supported, in part, by grants-in-aid for Scientific Research from the Ministry of Education, Culture, Sports, Science and Technology of Japan [grant number 19590867]; AstraZeneca Research grant 2007; the Mitsubishi Pharma Research Foundation; the Astellas Foundation for Research on Metabolic Disorders; and the Kimura Memorial Heart Foundation Research Grant for 2009.

REFERENCES

1 Winblad, B., Kilander, L., Eriksson, S., Minthon, L., Batsman, S., Wetterholm, A. L., Jansson-Blixt, C. and Haglund, A. (2006) Donepezil in patients with severe Alzheimer's disease: double-blind, parallel-group, placebo-controlled study. Lancet **367**, 1057–1065
2 Reale, M., Iarlori, C., Gambi, F., Lucci, I., Salvatore, M. and Gambi, D. (2005) Acetylcholinesterase inhibitors effects on oncostatin-M, interleukin-1β and interleukin-6 release from lymphocytes of Alzheimer's disease patients. Exp. Gerontol. **40**, 165–171
3 Rosas-Ballina, M. and Tracey, K. J. (2009) Cholinergic control of inflammation. J. Intern. Med. **265**, 663–679
4 Borovikova, L. V., Ivanova, S., Zhang, M., Yang, H., Botchkina, G. I., Watkins, L. R., Wang, H., Abumrad, N., Eaton, J. W. and Tracey, K. J. (2000) Vagus nerve stimulation attenuates the systemic inflammatory response to endotoxin. Nature **405**, 458–462
5 Wang, H., Liao, H., Ochani, M., Justiniani, M., Lin, X., Yang, L., Al-Abed, Y., Wang, H., Metz, C., Miller, E. J. et al. (2004) Cholinergic agonists inhibit HMGB1 release and improve survival in experimental sepsis. Nat. Med. **10**, 1216–1221
6 de Jonge, W. J., van der Zanden, E. P., The, F. O., Bijlsma, M., van Westerloo, D. J., Bennink, R. J., Berthoud, H. R., Uematsu, S., Akira, S., van den Wijngaard, R. M. and Boeckxstaens, G. E. (2005) Stimulation of the vagus nerve attenuates macrophage activation by activating the Jak2-STAT3 signaling pathway. Nat. Immunol. **6**, 844–851
7 Taqueti, V. R., Mitchell, R. N. and Lichtman, A. H. (2006) Protecting the pump: controlling myocardial inflammatory responses. Annu. Rev. Physiol. **68**, 67–95
8 Hoefer, I. E., van Royen, N., Rectenwald, J. E., Bray, E. J., Abouhamze, Z., Moldawer, L. L., Voskuil, M., Piek, J. J., Buschmann, I. R. and Ozaki, C. K. (2002) Direct evidence for tumor necrosis factor-alpha signaling in arteriogenesis. Circulation. **105**, 1639–1641
9 Carmeliet, P. (2003) Angiogenesis in health and disease. Nat. Med. **9**, 653–660
10 Tateno, K., Minamino, T., Toko, H., Akazawa, H., Shimizu, N., Takeda, S., Kunieda, T., Miyauchi, H., Oyama, T., Matsuura, K. et al. (2006) Critical roles of muscle-secreted angiogenic factors in therapeutic neovascularization. Circ. Res. **98**, 1194–1202
11 Bhat, R. V., Turner, S. L., Marks, M. J. and Collins, A. C. (1990) Selective changes in sensitivity to cholinergic agonists and receptor changes elicited by continuous physostigmine infusion. J. Pharmacol. Exp. Ther. **255**, 187–196
12 Saxena, G., Singh, S. P., Agrawal, R. and Nath, C. (2008) Effect of donepezil and tacrine on oxidative stress in intracerebral streptozotocin-induced model of dementia in mice. Eur. J. Pharmacol. **581**, 283–289
13 Heeschen, C., Jang, J. J., Weis, M., Pathak, A., Kaji, S., Hu, R. S., Tsao, P. S., Johnson, F. L. and Cooke, J. P. (2001) Nicotine stimulates angiogenesis and promotes tumor growth and atherosclerosis. Nat. Med. **7**, 833–839
14 Choi, K. M., Zhu, J., Stoltz, G. J., Vernino, S., Camilleri, M., Szurszewski, J. H., Gibbons, S. J. and Farrugia, G. (2007) Determination of gastric emptying in nonobese diabetic mice. Am. J. Physiol. Gastrointest. Liver Physiol. **293**, G1039–G1045

15 Baschong, W., Suetterlin, R. and Laeng, R. H. (2001) Control of autofluorescence of archival formaldehyde-fixed, paraffin-embedded tissue in confocal laser scanning microscopy (CLSM). J. Histochem. Cytochem. **49**, 1565–1572
16 Imayama, I., Ichiki, T., Inanaga, K., Ohtsubo, H., Fukuyama, K., Ono, H., Hashiguchi, Y. and Sunagawa, K. (2006) Telmisartan downregulates angiotensin II type 1 receptor through activation of peroxisome proliferator-activated receptor γ. Cardiovasc. Res. **72**, 184–190
17 Amano, K., Okigaki, M., Adachi, Y., Fujiyama, S., Mori, Y., Kosaki, A., Iwasaka, T. and Matsubara, H. (2004) Mechanism for IL-1β-mediated neovascularization unmasked by IL-1β knock-out mice. J. Mol. Cell. Cardiol. **36**, 469–480
18 Turner, N. A., Mughal, R. S., Warburton, P., O'Regan, D. J., Ball, S. G. and Porter, K. E. (2007) Mechanism of TNF-α -induced IL-1α, IL-1β and IL-6 expression in human cardiac fibroblasts: effects of statins and thiazolidinediones. Cardiovasc. Res. **76**, 81–90
19 Singh, S., Loke, Y. K. and Furberg, C. D. (2008) Inhaled anticholinergics and risk of major adverse cardiovascular events in patients with chronic obstructive pulmonary disease: a systematic review and meta-analysis. JAMA, J. Am. Med. Assoc. **300**, 1439–1450
20 Tashkin, D. P., Celli, B., Senn, S., Burkhart, D., Kesten, S., Menjoge, S. and Decramer, M. (2008) A 4-year trial of tiotropium in chronic obstructive pulmonary disease. N. Engl. J. Med. **359**, 1543–1554
21 Wessler, I., Kirkpatrick, C. J. and Racke, K. (1999) The cholinergic 'pitfall': acetylcholine, a universal cell molecule in biological systems, including humans. Clin. Exp. Pharmacol. Physiol. **26**, 198–205
22 Hamann, M., Chamoin, M. C., Portalier, P., Bernheim, L., Baroffio, A., Widmer, H., Bader, C. R. and Ternaux, J. P. (1995) Synthesis and release of an acetylcholine-like compound by human myoblasts and myotubes. J. Physiol. **489**, 791–803
23 Pavlov, V. A., Ochani, M., Gallowitsch-Puerta, M., Ochani, K., Huston, J. M., Czura, C. J., Al-Abed, Y. and Tracey, K. J. (2006) Central muscarinic cholinergic regulation of the systemic inflammatory response during endotoxemia. Proc. Natl. Acad. Sci. U.S.A. **103**, 5219–5223
24 Deguchi, J. O., Yamazaki, H., Aikawa, E. and Aikawa, M. (2009) Chronic hypoxia activates the Akt and β-catenin pathways in human macrophages. Arterioscler., Thromb., Vasc. Biol. **29**, 1664–1670
25 Kakinuma, Y., Furihata, M., Akiyama, T., Arikawa, M., Handa, T., Katare, R. G. and Sato, T. (2010) Donepezil, an acetylcholinesterase inhibitor against Alzheimer's dementia, promotes angiogenesis in an ischemic hindlimb model. J. Mol. Cell. Cardiol. **48**, 680–693
26 Kim, J. A., March, K., Chae, H. D., Johnstone, B., Park, S. J., Cook, T., Merfeld-Clauss, S. and Broxmeyer, H. E. (2010) Muscle-derived $Gr1^{dim}CD11b^{+}$ cells enhance neovascularization in an ischemic hind limb mouse model. Blood **116**, 1623–1626
27 Qi, X., Okamoto, Y., Murakawa, T., Wang, F., Oyama, O., Ohkawa, R., Yoshioka, K., Du, W., Sugimoto, N., Yatomi, Y. et al. (2010) Sustained delivery of sphingosine-1-phosphate using poly(lactic-co-glycolic acid)-based microparticles stimulates Akt/ERK-eNOS mediated angiogenesis and vascular maturation restoring blood flow in ischemic limbs of mice. Eur. J. Pharmacol. **634**, 121–131

Received 6 December 2011/26 January 2012; accepted 28 February 2012
Published as Immediate Publication 28 February 2012, doi:10.1042/CS20110633

Clinical Science (2012) **123**, 241–249 (Printed in Great Britain) doi:10.1042/CS20110633

online data

SUPPLEMENTARY ONLINE DATA

Acetylcholinesterase inhibitors attenuate angiogenesis

Ryohei MIYAZAKI*, Toshihiro ICHIKI*†, Toru HASHIMOTO*, Jiro IKEDA*, Aya KAMIHARAGUCHI*, Eriko NARABAYASHI*, Hirohide MATSUURA*, Kotaro TAKEDA*† and Kenji SUNAGAWA*

*Departments of Cardiovascular Medicine, Kyushu University Graduate School of Medical Sciences, Fukuoka, Japan, and †Advanced Therapeutics for Cardiovascular Diseases, Kyushu University Graduate School of Medical Sciences, Fukuoka, Japan

Table S1 Sequences of the primers used in real-time PCR

Angpt 1 and 2, angiopoietin 1 and 2; PlGF, placental growth factor.

	Sequence (5′→3′)	
Gene	Forward	Reverse
TNFα	AAGCCTGTAGCCCACGTCGTA	GGCACCACTAGTTGGTTGTCTTTG
IL-1β	GCAACTGTTCCTGAACTCAACT	ATCTTTTGGGGTCCGTCAACT
IL-6	CCACTTCACAAGTCGGAGGCTTA	GCAAGTGCATCATCGTTGTTCATAC
VEGF	GCACATAGGAGAGATGAGCTTCC	CTCCGCTCTGAACAAGGCT
Angpt1	CCGAGCCTACTCACAGTACGACAG	AAATCGGCACCGTGTAAGATCAA
Angpt2	GGACAGTCATCCAACACCGAGA	CAAACTCATTGCCCAGCCAGTA
PDGF	CAAAGGCAAGCACCGAAAGTTTA	CCGAATCAGGCATCGAGACA
bFGF	GTGCCAACCGGTACCTTGCTA	TCAGTGCCACATACCAACTGGAG
PlGF	CCTGTCTGCTGGGAACAACTCA	CACCTCATCAGGGTATTCATCCAAG
CD3ε	CACTCTGGGCTTGCTGATGG	TCATAGTCTGGGTTGGGAACAGG
F4/80	GAGATTGTGGAAGCATCCGAGAC	GATGACTGTACCCACATGGCTGA
β-Actin	GGCTGTATTCCCCTCCATCG	CCAGTTGGTAACAATGCCATG

Table S2 HR, BP and body weight in the experimental groups

Results are means ± S.E.M. *$P < 0.05$ compared with control.

Group	HR (beats/min)	SBP (mmHg)	Body weight (g)
Control	555 ± 34	101 ± 10	24.8 ± 0.8
Donepezil	452 ± 31*	97 ± 6	23.3 ± 0.3
Physostigmine	501 ± 20	100 ± 2	23.2 ± 0.7
Nicotine	522 ± 56	101 ± 17	24.3 ± 1.9
Betahnechol	472 ± 47	95 ± 8	23.8 ± 1.9

Table S3 HR, BP and body weight in the experimental groups treated with donepezil with or without IL-1β

Results are means ± S.E.M.

Group	HR (beats/min)	SBP (mmHg)	Body weight (g)
Control + PBS	531 ± 21	104 ± 6	24.1 ± 0.5
Donepezil + PBS	490 ± 26	100 ± 4	23.7 ± 1.7
Donepezil + IL-1β	501 ± 8	105 ± 3	23.6 ± 0.6

Received 6 December 2011/26 January 2012; accepted 28 February 2012
Published as Immediate Publication 28 February 2012, doi:10.1042/CS20110633

Correspondence: Professor Toshihiro Ichiki (email ichiki@cardiol.med.kyushu-u.ac.jp).

INTERNAL MEDICINE

□ ORIGINAL ARTICLE □

Usefulness of Non-contact Mapping for Radiofrequency Catheter Ablation of Inappropriate Sinus Tachycardia: New Procedural Strategy and Long-term Clinical Outcome

Masao Takemoto[1], Yasushi Mukai[1], Shujiro Inoue[1], Tetsuya Matoba[1], Mari Nishizaka[1], Tomomi Ide[1], Akiko Chishaki[2] and Kenji Sunagawa[1]

Abstract

Objectives The present study evaluated the clinical benefits of a new therapeutic method of radiofrequency catheter ablation (RFCA) using an EnSite system for inappropriate sinus tachycardia (IST).

Materials and Methods Six patients with debilitating IST underwent RFCA using EnSite. Using the beta-adrenergic blocker and agonist, the heart rate was controlled between 70 to 150 bpm before and after the RFCA. The areas of the breakout sites (BOSs) were clearly distinguished between those from the normal P-wave zones during rates of less than 100 bpm and those from more upper rate sites during rates of more than 100 bpm using the EnSite system, in accordance with the appearance of tall P-waves (tall P-wave zone) in the IST patients. This was selected as the target for ablation.

Results After the RFCA, the BOSs observed during heart rates of more than 100 bpm moved completely from the tall P-wave zone to the normal P-wave zone in the IST patients. The total number of heart beats and average heart beat on the 24-h Holter monitoring decreased statistically from that before the RFCA to that after, and no adverse heart rate responses was observed after the RFCA. Before the RFCA, the brain natriuretic peptide was elevated, New York Heart Association functional class was worse, and there was an impaired exercise tolerance observed with exercise electrocardiogram testing. The RFCA for the IST significantly improved those parameters.

Conclusion This new therapeutic method for IST using EnSite is effective and produces clinical benefits.

Key words: inappropriate sinus tachycardia, non-contact mapping, catheter ablation

(Intern Med 51: 357-362, 2012)
(DOI: 10.2169/internalmedicine.51.5882)

Introduction

Inappropriate sinus tachycardia (IST) is an uncommon clinical syndrome that is characterized by an elevated resting heart rate or disproportionate increase in the rate with minimal exertion (1). This condition is predominantly encountered in women and common symptoms include palpitations, presyncope/syncope, chest pain, dizziness, shortness of breath, anxiety and depression (2). Radiofrequency (RF) catheter ablation (RFCA) is an acceptable treatment modality for drug refractory IST, and several procedural strategies for sinus node (SN) modification have been described (1-3). Here we report our new observations using a non-contact mapping system, EnSite (St. Jude Medical, Minnetonka, MN, USA) in patients with drug refractory IST.

Materials and Methods

Study population and laboratory analysis

From 2006 to 2009, 6 consecutive patients (3 males and 3 females with a mean age of 43 ± 3 years old) with drug refractory (including beta-blockers, calcium-channel blockers,

[1]Department of Cardiovascular Medicine, Kyushu University Hospital, Japan and [2]Department of Health Sciences, Kyushu University Graduate School of Medical Sciences, Japan
Received for publication May 24, 2011; Accepted for publication November 2, 2011
Correspondence to Dr. Masao Takemoto, matakemo@cardiol.med.kyushu-u.ac.jp

and digitalis) IST underwent RFCA in our hospital. All patients had their history recorded, and underwent a physical examination, laboratory analysis, chest X-ray, 12-lead electrocardiogram, 24-h Holter monitoring, M-mode, two-dimensional and Doppler echocardiograms, and exercise electrocardiogram testing on admission or within at least 1 month before the admission, and 2 or 3 days after the RFCA. These examinations yielded no evidence of clinically overt structural heart disease, including coronary artery disease, valvular heart disease, congenital heart disease, LV hypertrophy, or RV abnormalities in any of the patients. The serum brain natriuretic peptide (BNP) concentration and New York Heart Association (NYHA) functional class were evaluated on admission and 6 to 12 months after the RFCA. The mean follow-up period was 29 ± 2 months.

Definition of IST

IST was defined as: 1) a P-wave axis and morphology during the tachycardia similar to that during sinus rhythm, and tall P-waves during the tachycardia which were at least 2-fold taller than those during sinus rhythm, especially in leads II, III, and aVF, 2) a heart rate of greater than 100 beats per minute (bpm) at rest or with minimal exertion, 3) exclusion of any secondary causes of tachycardia, 4) 24-h Holter monitoring demonstrating a mean heart rate of greater than 90 bpm, and 5) a heart rate of greater than 130 bpm within the first 90 seconds of a standard Bruce protocol on the treadmill test (1, 4, 5).

Mapping and catheter ablation procedure

All procedures were performed after written informed consent was obtained. The patients were studied in the fasting state without sedation. Antiarrhythmic drugs and beta-blockers were discontinued for at least five half-lives before the procedure. Under local anesthesia, two multipolar electrode catheters (St. Jude Medical, Tokyo, Japan) were placed percutaneously in the coronary sinus and high right atrium (RA), and His-bundle and right ventricle, respectively. A multielectrode array catheter utilizing EnSite 3.2 or EnSite 6.0J was positioned in the RA approximately at the level of the superior vena cava and RA junction with the distal end oriented superiorly using a guidewire (Fig. 1A, B). Thus, the distance between EnSite array and sinus node was less than 4 cm. A 7-F deflectable quadripolar ablation catheter, Ablaze or Fantasista (Japan Lifeline Co., Ltd., Tokyo, Japan) with a 4-mm-tip electrode was also introduced percutaneously into the RA, and the baseline RA geometry was acquired. An electrophysiological study (EPS) was performed before and after RFCA to verify the mechanism of arrhythmia and to exclude the coexistence of other arrhythmias.

Using an intravenous administration of the beta-adrenergic blocker, landiolol (5 to 40 μg/kg/min) and agonist, isoproterenol (ISP) (2 to 5 μg intravenous administration), the heart rate was controlled between 70 to 150 bpm before and after the RFCA. Then, the origins which indicated the SN during sinus rhythm and IST were defined as the earliest sites showing a single spot on the isopotential map and a QS pattern in the noncontact unipolar electrograms, as previously described (6). The breakout sites (BOSs) during sinus rhythm and IST were also defined as the earliest sites that showed an rS pattern with a sudden increase in the peak negative potential of the noncontact unipolar electrogram. These origins and BOSs were tagged for each heart rate on the RA geometry (Fig. 1C-H, 2A-J)). In all patients, compared to that during heart rates of less than 100 bpm with normal P-waves (normal P-wave zone), the BOSs steadily moved to more upper rate sites during heart rates of more than 100 bpm in accordance with the appearance of tall P-waves (tall P-wave zone) (Fig. 1C-J, 2A-J). The SN and BOSs within normal P-wave zones and tall P-wave zones could easily and clearly be separated by this method. The RF energy was delivered to the tall P-wave zones, and not to the SN or normal P-wave zones, for 30 to 60 seconds with a preset temperature of 50℃ and power limit of 30W. In 4 of 6 patients, repetitive atrial response was observed. The average distance between SN and ablation site was 12.7 ± 0.7 mm. A successful RFCA was defined as that when the BOSs observed during heart rates of more than 100 bpm (100 to 150 bpm) moved completely from the tall P-wave zone to the normal P-wave zone (Fig. 2C, D, E, H-J) with and without the intravenous administration of isoproterenol in accordance with the abolishment of the tall P-waves on the 12-lead electrocardiogram during the RF energy delivery (arrows in Fig. 1K). All 12-lead electrocardiograms and the bipolar intracardiac electrograms (filtered at 30 to 400 Hz) were recorded and stored using a 96-channnel acquisition system (CardioLabEP, Prucka Engineering Inc., Houston, TX, USA). During the procedure, intravenous heparin was given as a 5,000-unit bolus dose.

Statistical analysis

The numerical results are expressed in the text as the mean ± standard deviation. Paired data were compared by a Student's *t* test. A value of $p<0.05$ was considered to indicate statistical significance.

Results

Patient characteristics

Although patients primarily women in this syndrome, 50% were male in this study. An RFCA procedure for IST was performed in 6 patients. Procedural success was achieved in all 6 (100%) of the patients. No patients suffered from any procedure-related complications including SN dysfunction (sick sinus syndrome), cardiac tamponade, diaphragmatic paralysis, or superior vena cava syndrome. During 1-year follow-up, no recurrence of IST was observed in any of the patients. However, in 1 of the 6 patients the IST recurred and that patient underwent a repeat RFCA with a successful result a year and a half after the first RFCA.

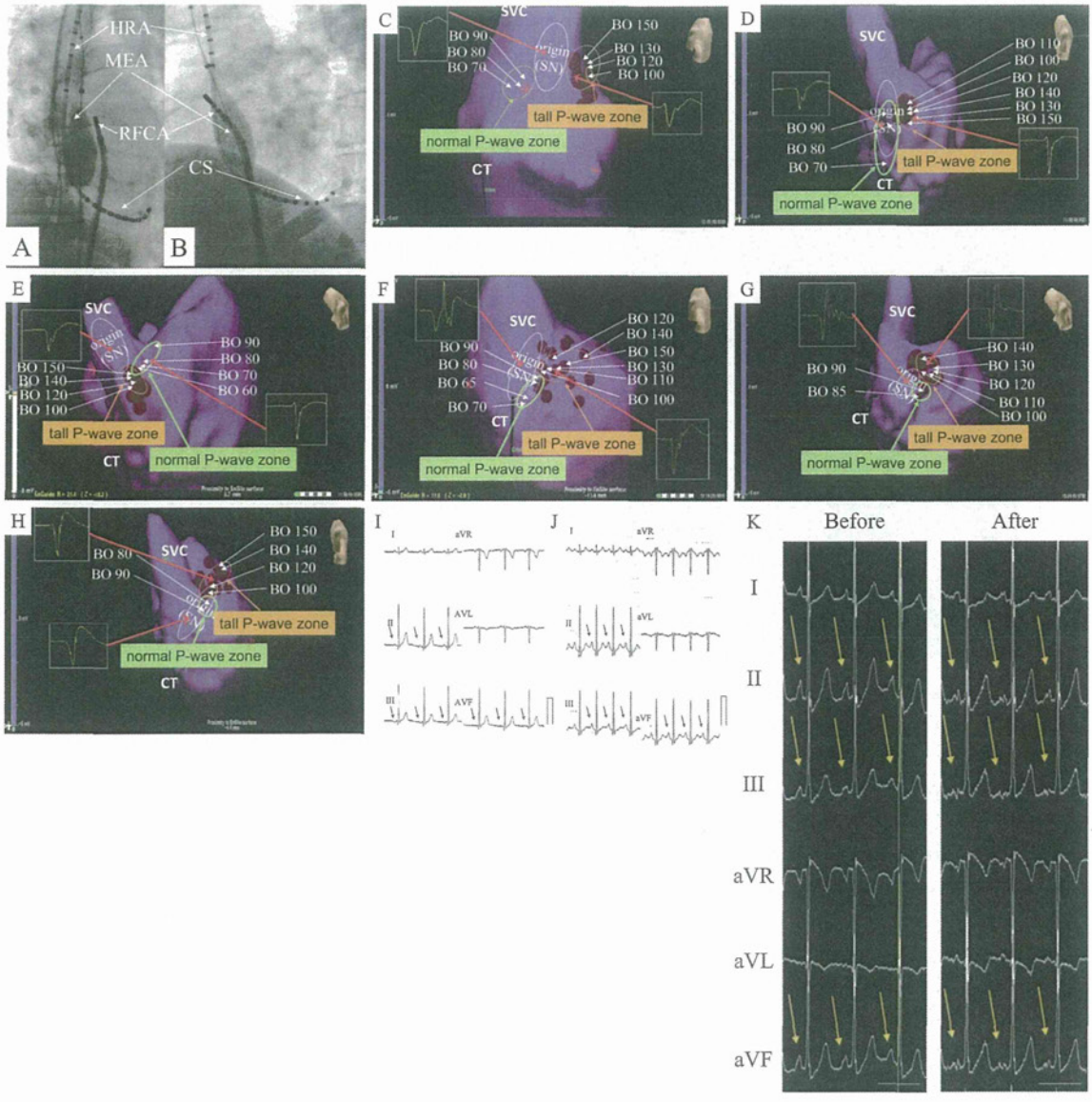

Figure 1. **Fluoroscopic images in the right (RAO; panel A) and left (LAO; panel B) anterior oblique views showing the location of the multipolar electrode catheters, multielectrode array (MEA) catheter, and radiofrequency ablation (RFCA) catheter placed in the high right atrium (HRA), coronary sinus (CS), and right atrium (RA) approximately at the level of the superior vena cava, respectively. The EnSite images of the RA in the RAO view of 6 cases (panel C-H) show the origin which indicates the location of the sinus node (SN) and breakout sites (BOSs) for each heart rate determined by the EnSite. The SN and BOSs, and normal P-wave zone and tall P-wave zone could easily and clearly be separated by the EnSite system. Compared to that for heart rates of less than 100 bpm associated with normal P-waves (arrows in panels I and J), the tall P-waves (arrows in panels J and K) were determined in the electrocardiogram, especially in leads II, III, aVF at heart rates of more than 100 bpm. Crista indicates the crista terminalis. SVC indicates superior vena cava. The bars in panel I and J indicate 1 mV. The bars in panel F indicate 400 ms.**

24-h Holter monitoring (Table 1)

The total number of heart beats and average heart beat statistically differed between that before and that after the RFCA ($p<0.01$) (Table 1). Although the heart rate was greater than 100 bpm at rest or with minimal exertion before the RFCA (Fig. 3A), an adverse heart rate response was not observed after the RFCA (Fig. 3B).

Serum BNP concentration and NYHA functional class

The serum BNP concentration and NYHA functional class were evaluated in all patients on admission and 6 to 12 months after the RFCA. The serum BNP was elevated before the RFCA. However, it significantly decreased 6 to 12 months after the RFCA ($p<0.05$) (Fig. 4A). The NYHA functional class was demonstrated to be significantly worse

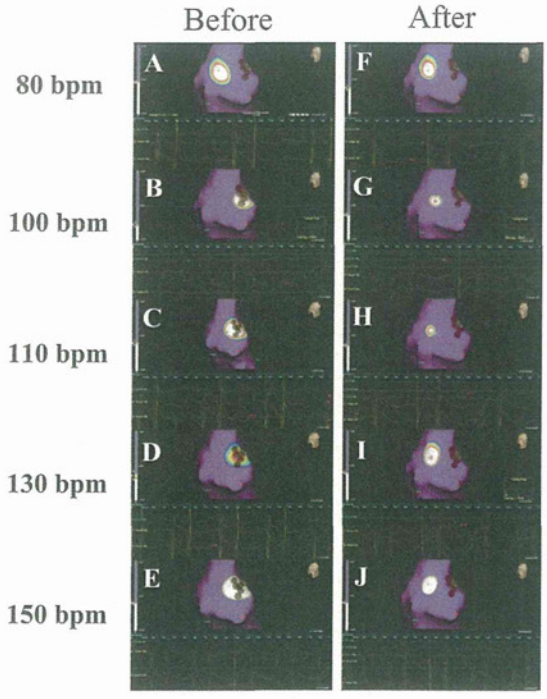

Figure 2. EnSite images of the right atrium in the right anterior oblique view. Before the radiofrequency catheter ablation (RFCA), compared to that for heart rates of less than 100 bpm associated with normal P-waves (normal P-wave zone), the breakout sites (BOSs) steadily moved to more upper sites during heart rates of more than 100 bpm associated with the appearance of tall P-waves (tall P-wave zone) (A-E). On the other hand, after the RFCA in the tall P-wave zone, the BOSs during heart rates of more than 100 bpm (100 to 150 bpm) moved completely from the tall P-wave zone to the normal P-wave zone with and without the intravenous administration of isoproterenol (F-J). The black lines on the geometry in panels A-J indicate the crista terminalis. RAA indicates right atrial appendage. The breakout sites (BOSs) during sinus rhythm and IST were usually defined as the earliest sites that showed an rS pattern with a sudden increase in the peak negative potential of the noncontact unipolar electrogram. However, QS patterns in the tracking virtual are seen in these figures. Since the origin is located in the epicardium or deep myocardium, the BOS was sometimes recoded as a QS pattern[15] in this present case. There is a possibility that the origin may be located adjacent to the BOS in this case.

before the RFCA (Fig. 4B). The RFCA significantly improved the NYHA functional class as compared to that before the intervention ($p<0.01$).

Exercise electrocardiogram testing (Table 1)

One of the 6 patients could not perform an exercise electrocardiogram test due to a gait disturbance caused by necrosis of the head of the femur. Compared to that before the RFCA, the resting heart rate significantly decreased after the RFCA ($p<0.05$). The time to achieve a heart rate of 130 bpm took significantly longer after the RFCA than before ($p<0.01$). Moreover, the RFCA significantly improved the exercise tolerance of the IST-patients ($p<0.05$).

Response to beta-adrenergic receptor stimulators (Table 1)

Before the RFCA, a low dose of ISP could steadily increase the patients' heart rate to 150 bpm. However, compared to that before the RFCA, a high dose of ISP was needed to increase the heart rate to 150 bpm ($p<0.01$) after the RFCA.

Patient symptoms and medications (Table 2)

On admission, all patients had IST-associated symptoms including palpitations (100%), general fatigue (83%), depression (67%) and fainting (33%). All patients had been taking antiarrhythmic agents before admission, such as beta-blockers (100%), calcium channel antagonists (33%) and digitalis (17%). However, those agents were not sufficiently effective in eliminating the IST-associated tachycardia and symptoms. All of the patients with a successful procedure reported the absence of any IST-associated tachycardia or symptoms after the RFCA. In 4 of the 6 patients it was possible to discontinue those antiarrhythmic agents. Two of the 6 patients continued to receive the beta-blockers for their hypertension.

Discussion

Major findings and clinical implications

The major findings of this study are as follows: 1) in a short time EnSite could steadily and clearly separate the SN, normal P-wave zone, and tall P-wave zone which was the targeted site of the RFCA (Fig. 1C-H, 2A-J), 2) the RFCA could easily and efficaciously treat the IST without any complications, and 3) all patients were free from any further IST-associated tachycardia (Fig. 3A, B) or symptoms (Table 2) in accordance with a decrease in their heart rate (Table 1), and experienced a dramatic improvement in the inappropriate increase in their heart rate with minimal exertion (Table 1), serum BNP level (Fig. 4A), NYHA functional class (Fig. 4B), and exercise tolerance (Table 1). Some previous studies demonstrated that the recurrence rate was 20 to 50% and some patients underwent a pacemaker implantation (1, 3, 7-9). However, with this method, the recurrence rate was only 1 out of 6 patients (17%) during a mean follow-up period of 29 ± 2 months. The characteristic point of this method which differs from that of the previous studies is that the target site of the RFCA was the BOSs in the tall P-wave zone, and not the SN. Thus, the RF energy could safely and easily be delivered at the target sites (BOSs) without any complications. As a result, this method could achieve an acceptable long-term clinical outcome. This method should be a new safe and effective procedural strategy for IST.

Table 1. Parameters before and after Radiofrequency Catheter Ablation

	Before	After
24-h Holter Monitoring Analysis (n=6)		
total HB (x10^3 beats/day)	134 ± 2	113 ± 2**
average HB (beats/minute)	93 ± 1	79 ± 1**
Exercise Eelectrocardiogram Testing Analysis (n=5)		
Resting HR (beats/minute)	108 ± 2	95 ± 2 *
Time-HR130 (seconds)	76 ± 5	212 ± 5**
Exercise tolerance (Mets)	6.8 ± 0.4	9.3 ± 0.6*
Response to Beta-adrenergic Receptor Stimulator (n=6)		
ISP dose achieved HR150 bpm (μg)	2.8 ± 0.2	4.8 ± 0.3**

**p<0.01, *p<0.05 versus before RFCA, HB = heart beats; HR = heart rate; Time-HR130 = time achieved 130 bpm of the heart rate; ISP = isoproterenol.

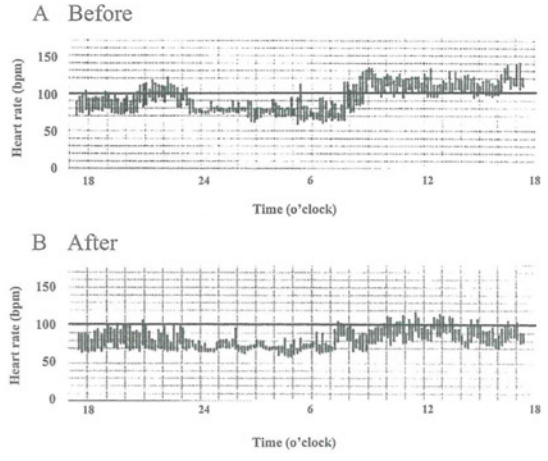

Figure 3. The 24-h Holter monitoring before and after the radiofrequency catheter ablation (RFCA). The heart rate was greater than 100 bpm at rest or with minimal exertion before the RFCA (A). However, that adverse heart rate response was not observed after the RFCA (B).

Mechanism of IST

Although the mechanism(s) of IST has not been completely elucidated, several potential mechanisms have been raised include the following: 1) autonomic dysfunction including an increased sympathetic tone and/or receptor sensitivity, blunted parasympathetic tone, or sympathovagal imbalance (2, 10), 2) abnormal automaticity of the SN (2, 11), 3) an atrial tachycardia focus near the SN (2), and 4) dysautonomia involving the anterior right ganglionated plexi (ARGP) (12, 13).

In this method, the target of the RFCA sites was the BOSs in the tall P-wave zone, and not the SN, indicating that abnormal automaticity of the SN may not be the potential mechanism of IST (14). The distinction between a focal atrial tachycardia and IST is often difficult to make. Occasionally, this distinction can be made clinically in that atrial tachycardia may not be related to activity with an unpredictable onset of the tachycardia at rest or with minimal exertion. Moreover, the BOSs of the tachycardia shifts for each different heart rate. This point may differentiate IST from focal atrial tachycardia.

It has been reported that epinephrine injected into the ARGP, which is located in the fat pad at the base of the right pulmonary veins adjacent to the caudal end of the SN, induces IST, and ablation of the ARGP eliminated the IST without damaging the SN (12, 13). Since the ablation sites were near the SN in this study, it may be possible that the ARGP may have been ablated. However, we could not sufficiently explain why the BOSs moved from the tall P-wave zone to the normal P-wave zone. Further studies may be needed to explain this.

We assumed that two types of autonomic regulation may exist, because there are two types of BOSs, those associated with a tall P-wave zone and those with a normal P-wave zone. Since the response to beta-adrenergic receptor stimulators differed before and after the RFCA (Table 1), one type of autonomic regulation may be an increased sympathetic tone and/or receptor sensitivity. Thus, the ablation of these abnormal autonomic regulation sites may abolish the IST-associated tachycardia, and improve the response to beta-adrenergic receptor stimulators. As a result, the BOSs shifted from the tall-P wave zone, possibly autonomic regulation sites, to the normal P-wave zone, possibly normal autonomic regulation sites.

Limitation of this study

The patient number of this study is comparably small. This arrhythmia involves several mechanisms such as primary sinus node abnormality, depressed efferent cardiovagal reflex and beta-adrenergic hypersensitivity (11). Not all of the patients with this arrhythmia may show a similar response to landiolol or isoproterenol. The similar trend in the response might occur only in a small subgroup of patients with this arrhythmia.

Conclusion

Finally, this new therapeutic method for ablating IST using the EnSite system was effective and safe. Although IST is an uncommon clinical syndrome, it has disabling symptoms. Thus, physicians should be aware of this condition when examining a patient with a tachycardia characterized by an elevated resting heart rate or a disproportionate increase in the heart rate with minimal exertion. Since IST is often drug-refractory, RFCA utilizing EnSite may be considered as the first choice of therapy in such patients.

The authors state that they have no Conflict of Interest (COI).

Acknowledgement

We thank Ryoko Hayashi, Kou Adachi, Keiji Kobayashi, and Noriko Nakajima for their technical assistance with the electrophysiological studies in the cardiac catheterization laboratory, and John Martin for his linguistic assistance with this paper.

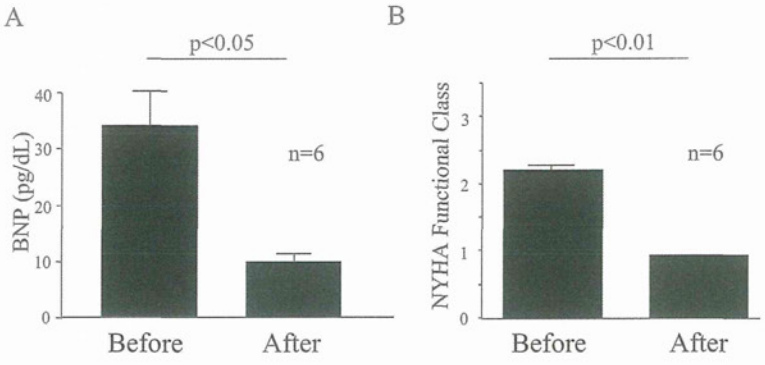

Figure 4. **The serum brain natriuretic peptide (BNP) concentration and New York Heart Association (NYHA) functional class before and 6 to 12 months after the radiofrequency catheter ablation (RFCA). The serum BNP level was elevated before the RFCA, however, it significantly decreased 6 to 12 months after the RFCA ($p<0.05$) (panel A). Although the NYHA functional class was demonstrated to be significantly worse before the RFCA (panel B), the RFCA significantly improved the NYHA functional class as compared to that before the intervention ($p<0.01$).**

Table 2. **Patient Symptoms and Medications before and after Radiofrequency Catheter Ablation**

	Before	After
Symptoms		
palpitations	100%	0%
general fatigue	83%	0%
depression	67%	0%
fainting	33%	0%
Medications		
beta-blockers	100%	33%
calcium-channel blockers	33%	0%
digitalis	17%	0%

References

1. Marrouche NF, Beheiry S, Tomassoni G, et al. Three-dimensional nonfluoroscopic mapping and ablation of inappropriate sinus tachycardia. Procedural strategies and long-term outcome. J Am Coll Cardiol **39**: 1046-1054, 2002.
2. Shen WK. How to manage patients with inappropriate sinus tachycardia. Heart Rhythm **2**: 1015-1019, 2005.
3. Lin D, Garcia F, Jacobson J, et al. Use of noncontact mapping and saline-cooled ablation catheter for sinus node modification in medically refractory inappropriate sinus tachycardia. Pacing Clin Electrophysiol **30**: 236-242, 2007.
4. Wilson RF, Johnson TH, Haidet GC, et al. Sympathetic reinnervation of the sinus node and exercise hemodynamics after cardiac transplantation. Circulation **101**: 2727-2733, 2000.
5. Lee RJ, Shinbane JS. Inappropriate sinus tachycardia. Diagnosis and treatment. Cardiol Clin **15**: 599-605, 1997.
6. Higa S, Tai CT, Lin YJ, et al. Focal atrial tachycardia: new insight from noncontact mapping and catheter ablation. Circulation **109**: 84-91, 2004.
7. Man KC, Knight B, Tse HF, et al. Radiofrequency catheter ablation of inappropriate sinus tachycardia guided by activation mapping. J Am Coll Cardiol **35**: 451-457, 2000.
8. Leonelli F, Richey M, Beheiry S, et al. Tridimensional mapping: guided modification of the sinus node. J Cardiovasc Electrophysiol **9**: 1214-1217, 1998.
9. Lee RJ, Kalman JM, Fitzpatrick AP, et al. Radiofrequency catheter modification of the sinus node for "inappropriate" sinus tachycardia. Circulation **92**: 2919-2928, 1995.
10. Bauernfeind RA, Amat YLF, Dhingra RC, et al. Chronic nonparoxysmal sinus tachycardia in otherwise healthy persons. Ann Intern Med **91**: 702-710, 1979.
11. Morillo CA, Klein GJ, Thakur RK, et al. Mechanism of 'inappropriate' sinus tachycardia. Role of sympathovagal balance. Circulation **90**: 873-877, 1994.
12. Zhou J, Scherlag BJ, Niu G, et al. Anatomy and physiology of the right interganglionic nerve: implications for the pathophysiology of inappropriate sinus tachycardia. J Cardiovasc Electrophysiol **19**: 971-976, 2008.
13. Scherlag BJ, Yamanashi WS, Amin R, et al. Experimental model of inappropriate sinus tachycardia: initiation and ablation. J Interv Card Electrophysiol **13**: 21-29, 2005.
14. Stiles MK, Brooks AG, Roberts-Thomson KC, et al. High-density mapping of the sinus node in humans: role of preferential pathways and the effect of remodeling. J Cardiovasc Electrophysiol **21**: 532-539, 2010.
15. Kaneko Y, Nakajima T, Saito A. The morphology of unipolar potentials predicts the depth of activation foci (abstr). Heart Rhythm **7**: S114, 2010.

Hypertension Research (2012) 35, 470–476

www.nature.com/hr

ORIGINAL ARTICLE

Activation of mineralocorticoid receptors in the rostral ventrolateral medulla is involved in hypertensive mechanisms in stroke-prone spontaneously hypertensive rats

Toshiaki Nakagaki[1,2], Yoshitaka Hirooka[3], Ryuichi Matsukawa[1], Masaaki Nishihara[1], Masatsugu Nakano[1], Koji Ito[1], Sumio Hoka[2] and Kenji Sunagawa[1]

Mineralocorticoid receptor (MR) is recognized as a target for therapeutic intervention in hypertension and heart failure. MRs in the central nervous system are thought to have an important role in blood pressure regulation. Thus, we examined whether activation of the MR pathway in the rostral ventrolateral medulla (RVLM) of the brainstem contributes to the neural mechanism of hypertension in stroke-prone spontaneously hypertensive rats (SHRSPs). We microinjected eplerenone, aldosterone or Na^+-rich artificial cerebrospinal fluid (aCSF) into the RVLM of anesthetized Wistar–Kyoto (WKY) rats and SHRSPs. Arterial pressure (AP), heart rate (HR) and renal sympathetic nerve activity (RSNA) were recorded. The expressions of the MR protein and the serum- and glucocorticoid-regulated kinase protein (Sgk1), which is a marker of MR activity, in the RVLM were measured by western blot analysis. Bilateral microinjection of eplerenone into the RVLM decreased AP and RSNA in WKY rats and SHRSPs, and the decreases in those variables were significantly greater in SHRSPs than WKY rats. Microinjection of aldosterone or Na^+-rich aCSF into the RVLM increased AP and RSNA dose-dependently. The increases in those variables were significantly greater in SHRSPs than in WKY rats. The pressor responses of aldosterone or Na^+-rich aCSF were attenuated by the prior injection of eplerenone in SHRSPs. Sgk1 expression levels in the RVLM were significantly greater in SHRSPs than in WKY rats. These findings suggest that activation of MRs in the RVLM enhances sympathetic activity, thereby contributing to the neural mechanism of hypertension in the SHRSP.
Hypertension Research (2012) **35,** 470–476; doi:10.1038/hr.2011.220; published online 12 January 2012

Keywords: blood pressure; mineralocorticoid receptor; rostral ventrolateral medulla; sympathetic nervous system

INTRODUCTION

Accumulating evidence indicates that the sympathetic nervous system has an important role in the pathogenesis of hypertension.[1–3] Mineralocorticoid receptor (MR) is recognized as a target for therapeutic intervention in hypertension and heart failure.[4,5] The beneficial effects of the MR antagonist spironolactone or the more specific antagonist eplerenone on end-organ damage have been studied in animal models.[6–10] It has been reported that MRs regulate epithelial Na channels (ENaCs) that are important for the regulation of sodium transport and the maintenance of extracellular fluid volume and arterial pressure (AP) in the kidney.[11] Recent studies have reported the distribution of MRs or ENaCs in the choroid plexus, ependyma and neurons, such as those in the supraoptic nucleus, paraventricular nucleus and nucleus tractus solitarius.[12,13] In addition, the expression of MR mRNA has been reported in the brainstem,[14] including the rostral ventrolateral medulla (RVLM) and caudal ventrolateral medulla.[15,16] These findings suggest that MRs in the central nervous system, especially in neurons, regulate Na^+ influx via ENaCs, leading to hypertension and sympathoexcitation. However, it remains to be determined whether activation of MRs in the brainstem contributes to blood pressure regulation via the sympathetic nervous system.

The RVLM of the brainstem is one of the most important vasomotor centers that determines sympathetic nervous system activity, and it is essential for the maintenance of basal vasomotor tone.[3,17,18] There is a evidence that increased activity of the RVLM leads to sympathetic hyperactivity in various model of hypertension.[18–20] For example, both the pressor response to the microinjection of angiotensin II into the RVLM and the stimulation of AT_1

[1]Department of Cardiovascular Medicine, Kyushu University Graduate School of Medical Sciences, Fukuoka, Japan; [2]Department of Anesthesiology and Critical Care Medicine, Kyushu University Graduate School of Medical Sciences, Fukuoka, Japan and [3]Department of Advanced Cardiovascular Regulation and Therapeutics, Kyushu University Graduate School of Medical Sciences, Fukuoka, Japan
Correspondence: Dr Y Hirooka, Department of Advanced Cardiovascular Regulation and Therapeutics, Kyushu University Graduate School of Medical Sciences, 3-1-1 Maidashi, Higashi-ku, Fukuoka 812-8582, Japan.
E-mail: hyoshi@cardiol.med.kyushu-u.ac.jp
Received 16 September 2011; revised 9 October 2011; accepted 17 October 2011; published online 12 January 2012

receptors were enhanced in spontaneously hypertensive rats (SHRs).[21] The activation of endogenous AT_1 receptors has also been demonstrated in SHRs and stroke-prone spontaneously hypertensive rats (SHRSPs).[22,23] It has been reported that microinjection of aldosterone into the RVLM increases AP, and that the MR blocker spironolactone decreases AP.[24] The purpose of the present study was thus to determine whether the MR pathway in the RVLM contributes to the neural regulation of blood pressure through the sympathetic nervous system, and whether the activation of endogenous MRs in the RVLM leads to sympathetic hyperactivity and hypertension in SHRSPs. Furthermore, we examined neuronal sensitivity to Na^+ in the RVLM, because activation of MRs would induce ENaC upregulation.[11] SHRSPs are widely used as a model of hypertension, because they develop exaggerated blood pressure elevation with high sympathetic nervous system activity, thereby causing stoke and death.[23] In addition, oral administration of eplerenone prevented salt-induced cardiac fibrosis in SHRSPs.[6] For this purpose, we investigated the effects of aldosterone, Na^+-rich artificial cerebrospinal fluid (aCSF) and the MR blocker eplerenone administered into the RVLM on arterial blood pressure, heart rate (HR) and renal sympathetic nerve activity (RSNA). The expression of MRs and serum- and glucocorticoid-regulated kinase (Sgk1) expression levels, which indicate MR activity, were also evaluated.

METHODS

This study was reviewed and approved by the Animal Experiments Ethics Committee, Kyushu University Graduate School of Medical Sciences, and was conducted according to the Guidelines for Animal Experiments of Kyushu University.

Animals and general procedures

Male Wistar–Kyoto rats (WKY/Izm) and SHRSP/Izm (12–16 weeks old; SLC Japan, Hamamatsu, Japan) were used. Food and tap water were available ad libitum throughout the study. The rats were kept in a temperature- and humidity-controlled room with a 12-h light period between 0800 hours to 2000 hours.

Microinjection into the RVLM and recording of blood pressure, HR and RSNA

SHRSPs and WKY rats were initially anesthetized with sodium pentobarbital (50 mg kg^{-1} i.p., followed by a maintenance dosage of 20 mg kg^{-1} per h i.v.). A catheter was inserted into the femoral artery to record AP and HR. A tracheal cannula was connected to a ventilator, and the rats were artificially ventilated. Body temperature was monitored with a rectal thermometer and maintained in the range of 36.5–37.5 °C with a heating pad. The left renal nerve was exposed using a left retroperitoneal flank incision. A pair of stainless steel bipolar electrodes was placed beneath the renal nerve to record multifiber RSNA.[25] All signals were recorded on a computer using a PowerLab system (AD Instruments, Nagoya, Japan). The signal from the electrodes was amplified, passed through a band pass filter and then rectified and integrated (resetting every 0.1 s). The rats were placed in a stereotaxic frame, and the dorsal surface of the medulla was surgically exposed to allow for positioning of the microinjection pipettes in the RVLM (with the pipette angled rostrally 18 °C, 1.8 mm lateral, 3.5 mm below the calamus scriptorius), as previously described.[26] The microinjections (all microinjections were in a volume of 50–100 nl unless otherwise indicated) into the RVLM were made according to the following protocols: (1) bilateral microinjections of the MR blocker eplerenone (100 pmol each); (2) unilateral microinjection of aldosterone (10 pmol-1 nmol); (3) unilateral microinjection of aldosterone (100 pmol) 30 min after bilateral microinjections of eplerenone (100 pmol each); (4) unilateral microinjection of Na^+-rich aCSF (0.15–0.2 M); and (5) unilateral microinjection of Na^+-rich aCSF (0.2 M in 50 nl) 30 min after bilateral microinjections of eplerenone (100 pmol each).

aCSF (which contained (in mmol l^{-1}) 121 NaCl, 3.4 KCl, 1.2 $MgCl_2$, 0.6 NaH_2PO_4, 29 $NaHCO_3$ and 3.4 glucose) was used as a vehicle, and Na^+-rich aCSF was prepared by adjusting the [Na^+] of aCSF with additional NaCl.[27] Aldosterone was obtained from Sigma-Aldrich (St Louis, MO, USA). The MR blocker eplerenone was a gift from the Pfizer Pharmaceutical Company, (New York, NY, USA). Drug doses were based on previous reports[24,27] or our preliminary experiments. Before microinjection of the drugs, the RVLM was identified by monitoring the mean arterial pressure (MAP) after injecting a small dose (1 nmol) of L-glutamate. For bilateral injections, injections were first made on one side, and then the pipette was moved to the contralateral side; the two injections were made ~3 min apart.

Western blot analysis for the MR and Sgk1 in the RVLM

To obtain RVLM tissues, the rats were deeply anesthetized with sodium pentobarbital (100 mg kg^{-1} i.p.) and transcardially perfused with phosphate-buffered saline. The brain was quickly removed. The RVLM tissue was homogenized and then sonicated in a lysing buffer containing 40 mmol l^{-1} of 4-(2-hydroxyethyl)-1-piperazineethanesulfonic acid (HEPES), 1% Triton X-100, 10% glycerol, 1 mmol l^{-1} phenylmethanesulfonyl fluoride and 1 protease inhibitor cocktail tablet (Roche Diagnostics, Indianapolis, IN, USA). The tissue lysate was centrifuged at 6000 r.p.m. for 5 min at 4 °C in a microcentrifuge. The lysate was collected, and the protein concentration was determined using a bicinchoninic acid protein assay kit (Pierce, Rockford, IL, USA). Aliquots of protein (50 μg) from each sample were separated on a 7.5% sodium dodecyl sulfate-polyacrylamide gel. Subsequently, the separated proteins were transferred onto polyvinylidene difluoride membranes (Immobilon-P membrane; Millipore, Billerica, MA, USA). The membranes were incubated with goat IgG polyclonal antibody against MR (1:1000; Santa Cruz Biotechnology, Santa Cruz, CA, USA), with rabbit IgG polyclonal antibody against SGK1 (Abcam, Tokyo, Japan) and with rabbit IgG polyclonal antibody against glyceraldehyde-3-phosphate dehydrogenase (1:1000; Santa Cruz Biotechnology) for 24 to 48 h. The membranes were then washed and incubated with horseradish peroxidase-conjugated horse anti-goat IgG or anti-rabbit antibody (1:10000; Santa Cruz Biotechnology) for 40 min. Immunoreactivity was detected by autoradiography using enhanced chemiluminescence and a western blotting detection kit (Amersham, Piscataway, NJ, USA).

Statistical analysis

All values are expressed as the mean ± s.e.m. The changes in MAP, HR and RSNA values during the eplerenone microinjection studies and the MR and Sgk1 receptor expression were compared between SHRSPs and WKY rats using an unpaired *t*-test. Intergroup differences in MAP and RSNA after aldosterone and Na^+-rich aCSF microinjection were compared using two-way analysis of variance. *P* values of <0.05 were considered statistically significant.

RESULTS

Effect of blockade of MR in the RVLM on arterial pressure, HR and RSNA

The basal MAP and HR were significantly higher in SHRSPs than in WKY rats (183.1 ± 4.1 *vs.* 103.2 ± 2.7 mm Hg, 355.7 ± 3.1 *vs.* 318.1 ± 3.3 b.p.m., $P<0.01$, $n=5$ for each). Bilateral microinjection of the MR blocker eplerenone into the RVLM induced a significant decrease in MAP, HR and RSNA in both SHRSPs and WKY rats. The magnitudes of the decreases in AP and RSNA were significantly greater in SHRSPs than in WKY rats (ΔMAP, −31.5 ± 2.7 *vs.* −12.0 ± 1.2 mm Hg, $P< 0.01$; RSNA Δbaseline, −14.6 ± 2.1 *vs.* −4.3 ± 0.5%, $P<0.01$, $n=5$ for each; Figures 1a and b). In contrast, the decrease in HR was not significantly different between SHRSPs and WKY rats (ΔHR, −22.9 ± 7.8 *vs.* −17.4 ± 9.2 b.p.m.; NS, $n=5$). These changes occurred several minutes after injection, peaked at 40–60 min, and gradually recovered over time, but they lasted more than 2 h.

Effect of microinjection of aldosterone into the RVLM on arterial pressure, HR and RSNA

The basal MAP and HR were significantly higher in SHRSPs than in WKY rats (185.7. ± 5.6 *vs.* 91.9 ± 2.7 mm Hg, 356.5 ± 4.2 *vs.*

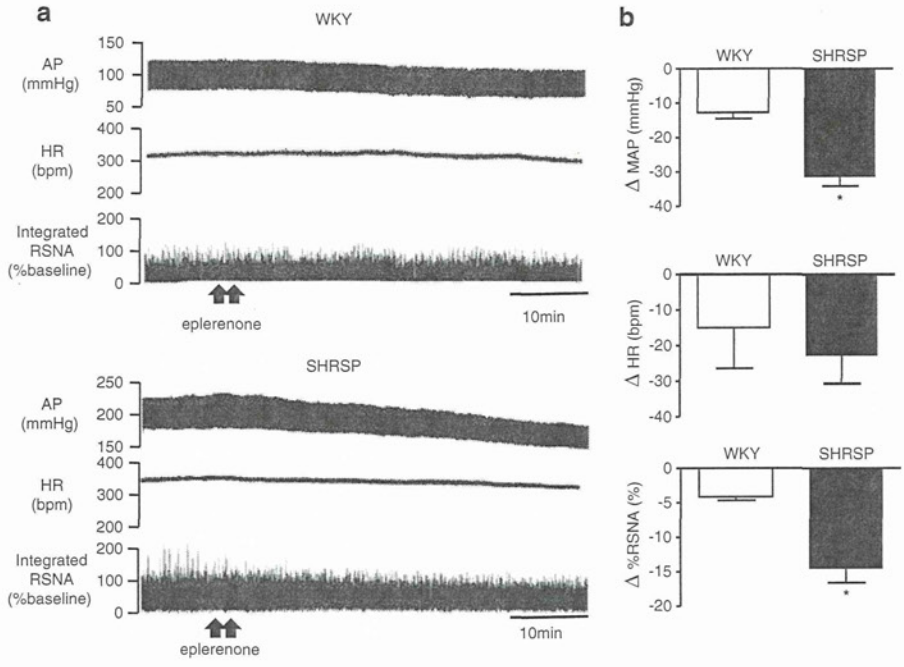

Figure 1 The responses of arterial pressure (AP), heart rate (HR) and renal sympathetic nerve activity (RSNA) to bilateral microinjection of the mineralocorticoid receptor (MR) blocker eplerenone into the RVLM of Wistar–Kyoto (WKY) rats and stroke-prone spontaneously hypertensive rats (SHRSPs). (**a**) Raw data of the changes in AP, HR and RSNA evoked by bilateral microinjection of eplerenone in WKY rats and SHRSPs. (**b**) Group data of the changes in mean arterial pressure (MAP), HR and RSNA in response to bilateral microinjection of eplerenone (100 pmol). Values are expressed as the mean ± s.e.m. $^*P<0.05$ ($n=5$ for each).

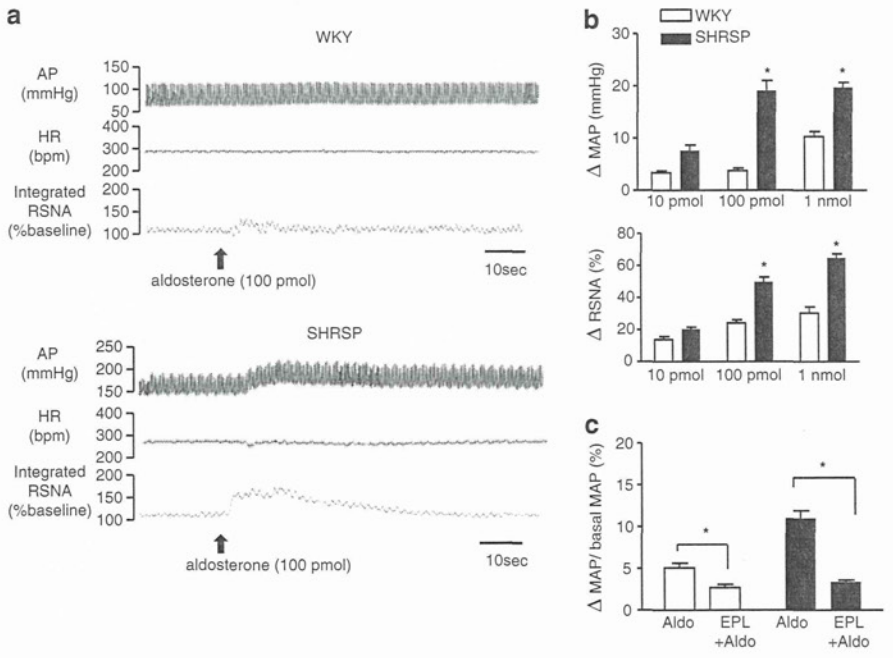

Figure 2 The responses of arterial pressure (AP), heart rate (HR) and renal sympathetic nerve activity (RSNA) to microinjection of aldosterone into the rostral ventrolateral medulla (RVLM). (**a**) Raw data of the changes in AP, HR and RSNA after unilateral injection of aldosterone (10 pmol-1 nmol) into the RVLM in Wistar–Kyoto (WKY) rats and stroke-prone spontaneously hypertensive rats (SHRSPs). (**b**) Group data of the changes in mean arterial pressure (MAP) and HR evoked by unilateral microinjection of aldosterone (10 pmol–1 nmol) into the RVLM in WKY rats and SHRSPs. (**c**) Group data of the changes in MAP in response to microinjection of aldosterone (100 pmol) without pretreatment (Aldo) and microinjection of aldosterone with pretreatment of eplerenone (100 pmol) (Aldo + EPL) in WKY rats and SHRSPs. Values are expressed as the mean ± s.e.m. $^*P<0.05$ ($n=4$ for each).

302 ± 5.1 b.p.m., $P<0.01$, $n=4$ for each). Unilateral microinjection of aldosterone into the RVLM significantly increased MAP and RSNA in both SHRSPs and WKY rats. The pressor response induced by aldosterone occurred in a dose-dependent manner (Figures 2a and b). No significant changes in HR were observed in either strain of rats (data not shown). The magnitude of the increases in these variables was significantly greater in SHRSPs than in WKY rats ($P<0.05$, $n=4$ for each; Figure 2b). Pretreatment with eplerenone nearly prevented the aldosterone-induced pressor responses in SHRSPs and WKY rats. However, the blocking effect of MRs was significantly greater in SHRSPs ($P<0.05$, $n=5$ for each; Figure 2c).

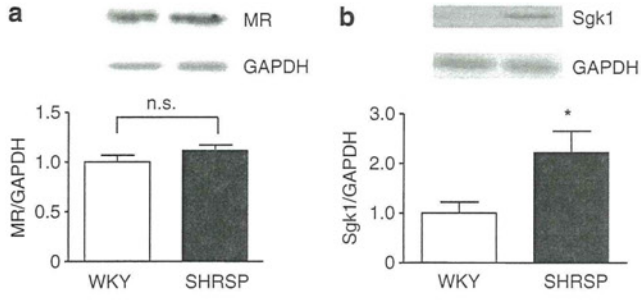

Figure 3 Western blot analysis demonstrating (**a**) mineralocorticoid receptor (MR) and (**b**) serum- and glucocorticoid-regulated kinase (Sgk1) expression in the rostral ventrolateral medulla (RVLM) in 12-week-old Wistar–Kyoto (WKY) rats and stroke-prone spontaneously hypertensive rats (SHRSPs). The densitometric average was normalized to the values obtained from the analysis of glyceraldehyde-3-phosphate dehydrogenase (GAPDH) as an internal control. Expressions are shown relative to those seen in WKY rats, which were assigned a value of 1. Values are expressed as the mean ± s.e.m. *$P<0.05$ ($n=4$ for each).

MR and Sgk1 expression levels in the RVLM

The protein expression levels of MRs in the RVLM did not differ between SHRSPs and WKY rats. However, the levels of Sgk1, which is induced by MRs and is a marker of the activity of MRs, were significantly greater in SHRSPs than in WKY rats ($P<0.05$, $n=4$ for each; Figure 3).

Effect of microinjection of Na^+-rich aCSF into the RVLM on arterial pressure, HR and RSNA

Similarly, the basal MAP and HR were significantly higher in SHRSPs than in WKY rats (180.8. ± 4.1 *vs.* 87.1 ± 9.9 mm Hg, 357.9 ± 5.6 *vs.* 312.5 ± 6.4 b.p.m., $P<0.01$, $n=5$ for each). Microinjection of Na^+-rich aCSF into the RVLM increased both MAP and RSNA in a dose-dependent manner (Figures 4a and b), whereas microinjection of 0.15 M aCSF into the RVLM caused no significant changes in MAP, HR or RSNA. The magnitudes of the increases in these variables were significantly greater in SHRSPs than in WKY rats ($P<0.05$, $n=5$ for each; Figure 4b). In addition, pretreatment with bilateral microinjection of eplerenone into the RVLM significantly attenuated the Na^+-rich aCSF-induced pressor responses in SHRSPs, but did not significantly change them in WKY rats ($P<0.05$, $n=5$ for each; Figure 4c).

DISCUSSION

The findings of this study were as follows: (1) blockade of MRs in the RVLM decreased MAP and RSNA in both SHRSPs and WKY rats, but the decreases were apparently greater in SHRSPs than in WKY rats; (2) microinjection of aldosterone or Na^+-rich aCSF into the RVLM increased MAP via sympathetic nerve activity in both SHRSPs and WKY rats, but the increases were greater in SHRSPs than in WKY rats;

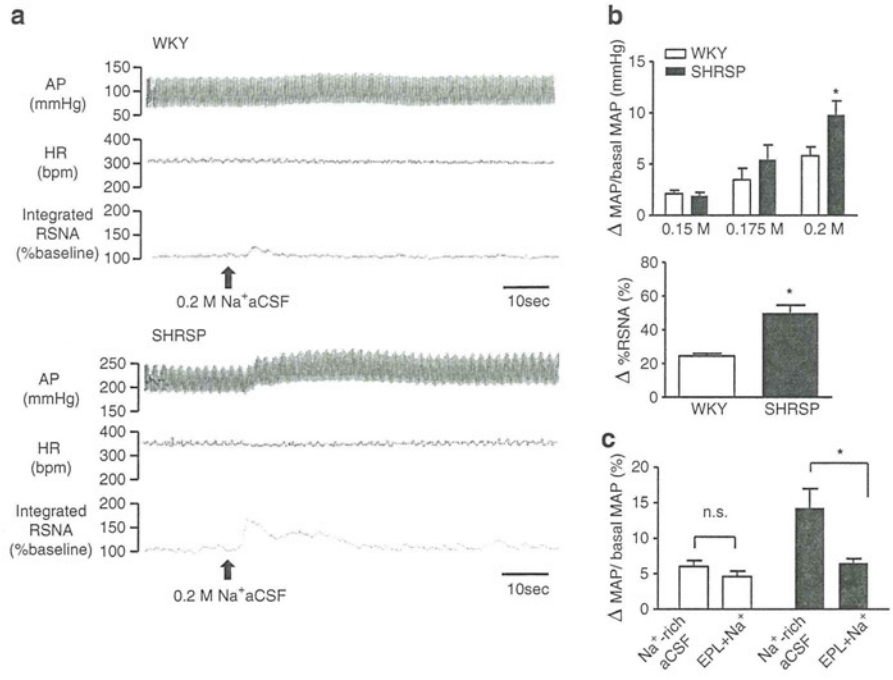

Figure 4 The response to unilateral microinjection of Na^+-rich artificial cerebrospinal fluid (aCSF) (0.15–0.2 M) into the rostral ventrolateral medulla (RVLM). (**a**) Raw data of the changes in mean arterial pressure (AP), heart rate (HR) and renal sympathetic nerve activity (RSNA) in Wistar–Kyoto (WKY) rats and stroke-prone spontaneously hypertensive rats (SHRSPs). (**b**) Group data of the changes in mean arterial pressure (MAP) and renal sympathetic nerve activity (RSNA) evoked by unilateral microinjection of Na^+-aCSF (0.2 M) into the RVLM in WKY rats and SHRSPs. (**c**) Group data of the changes in mean MAP in response to microinjection of Na^+-rich-aCSF (0.2 M) without pretreatment (Na^+-rich aCSF) and microinjection of Na^+ rich-aCSF (0.2 M) with pretreatment of eplerenone (100 pmol) (EPL + Na) in WKY rats and SHRSPs. Values are expressed as the mean ± s.e.m. *$P<0.05$ ($n=5$ for each).

(3) in SHRSPs, the prior injection of an MR blocker completely prevented the aldosterone-induced pressor response, but it only partially prevented the Na^+-rich aCSF-induced pressor response; and (4) the protein expression levels of MRs in the RVLM did not differ between SHRSPs and WKY rats. However, the Sgk1 expression levels were significantly greater in SHRSPs than in WKY rats. Taken together, our findings indicate that activation of MRs in the RVLM contributes to the neural mechanisms of hypertension in SHRSPs.

The most important finding of this study was that microinjection of the MR-specific blocker eplerenone into the RVLM induced decreases in MAP and RSNA in WKY rats and SHRSPs, and these decreases were greater in SHRSPs. MRs in the brain have been shown to be involved in sympathetic nerve activation in salt-sensitive hypertensive rats,[28] in a rat model of myocardial infarction[29] and in other salt-sensitive models.[30] The blockade of MRs in the brain has been suggested to decrease sympathetic nerve activation and result in a decrease in the blood pressure rise from high salt intake in salt-sensitive rats.[28] This decrease has also been associated with an improvement in the cardiac function of mice with pressure overload.[30] In the present study, we confirmed that endogenous blockade of MRs in the RVLM decreased blood pressure via sympathoinhibition, with greater decreases in SHRSPs. However, the decreases in HR were not significantly different, because it is difficult to assess HR in an acute experiment with anesthetics. To investigate the long-term effects of endogenous MR blockade on blood pressure or RSNA, we microinjected eplerenone into the RVLM bilaterally. It has been reported that Sgk1 is induced by aldosterone and upregulates ENaC levels and activity in the kidney,[11,31] and that this aldosterone-induced upregulation is dependent on MRs.[32] Therefore, these studies suggest that Sgk1 can be classified as an aldosterone-effector kinase and a marker of MR signaling. In the RVLM, the protein expression of MRs did not differ between the two strains, but Sgk1 was significantly higher in SHRSPs than in WKY rats. The enhanced protein expression of Sgk1 in SHRSPs in the present study might indicate an enhancement of MR stimulation in the RVLM. We observed that endogenous blockade of MRs by eplerenone induced a greater depressor response through sympathoinhibition in SHRSPs than in WKY rats, and exogenous stimulation of MR by aldosterone elicited a greater pressor response through sympathoexcitation in SHRSPs than in WKY rats. Altogether, these findings suggest that activation of MRs in the RVLM is enhanced and contributes to elevation of the AP in SHRSPs.

The effects of aldosterone have been ascribed to a genomic mechanism of binding to its receptors, followed by translocation of the steroid receptor complex to the nucleus, where it acts as a transcriptional regulator. However, recent studies suggest that effects may be because of non-genomic actions of aldosterone, which occur more rapidly after binding MRs.[33,34] For example, the rapid action of aldosterone in the kidney[33] or vasculature[34] has been demonstrated within a few minutes. Therefore, it is possible that acute inhibition of MR activation might be caused by non-genomic mechanism in the RVLM. However, we cannot exclude the possibility that genomic action is also involved in our observation, because the depressor response evoked by eplerenone lasted more than 2 h. In addition, it should be noted that the depressor and sympathoinhibitory responses occurred several minutes after the bilateral microinjection of eplerenone into the RVLM, and that the pressor and sympathoexcitatory responses occurred within seconds after the microinjection of aldosterone. In general, exogenously administered neurotransmitter/neuromodulators into the RVLM have been shown to elicit rapid action of blood pressure and sympathetic nerve activity. In contrast, the blockade of endogenous receptors in the RVLM gradually evokes the responses of blood pressure and sympathetic nerve activity.[35] In this context, the time course of the responses is not surprising, although we still do not have a clear explanation for this phenomenon. Further study is needed to clarify whether endogenous activation of MR is involved in hypertensive mechanisms both in the genomic and non-genomic action of aldosterone.

Our observations are consistent with previous reports that microinjection of aldosterone into the RVLM increases MAP.[24] It has been reported that intracerebroventricular (ICV) infusion of aldosterone increased MAP[36] and that these sympathoexcitatory and central pressor effects of aldosterone can be blocked by ICV infusion of an MR blocker. In the present study, microinjection of the MR blocker eplerenone into the RVLM also prevented an aldosterone-induced pressor response. These results suggest that aldosterone is likely to be an endogenous ligand of MRs in the RVLM. It has also been reported that central administration of aldosterone appears to depend on the MR–ENaC–ouabain pathway and, ultimately, AT_1 receptor stimulation.[37] The sympathoexcitatory and pressor responses to central infusion of aldosterone and Na^+-rich aCSF can be prevented by central infusion of the sodium channel blocker benzamil or an ouabain blocker,[27,38] and the pressor responses elicited by central infusion of aldosterone or ouabain can be blocked by an AT_1 blocker.[27,39] In the RVLM, microinjection of an ouabain-like compound[40] or angiotensin II[21] elicits a pressor response and sympathoexcitation. Collectively, these data suggest that aldosterone in the RVLM might activate central mechanism(s) involving the MR–ENaC–ouabain pathway, thereby causing sympathetic hyperactivity and hypertension.

Several studies have reported that aldosterone shows poor penetration of the blood-brain barrier compared with other steroid hormones.[12] However, the enzymes for steroid biosynthesis are present in the central nervous system[41] and RVLM,[15] and aldosterone can be detected in the tissues of various brain regions *in vitro*[41] and *in vivo*.[42] In particular, it should be noted that Gomez-Sanchez *et al.* reported that aldosterone was detectable in the whole brain of adrenalectomized rats, despite the fact that plasma aldosterone was undetectable.[41] These finding suggest that aldosterone is produced locally in the RVLM. In the present study, such locally produced aldosterone might have been enhanced and might have activated MRs in SHRSPs. Alternatively, there might be an aldosterone-independent MR activation pathway in the RVLM. It has been reported that MRs were activated by Rac1, which was independent of aldosterone in the kidney.[43] Further studies are needed to clarify the precise mechanisms involved in the activation of MR in the RVLM.

In this study, microinjection of Na^+-rich aCSF into the RVLM caused concentration-related increases in MAP and RSNA, whereas microinjection of 0.15 M aCSF at the same volume generated no significant increases. It has been reported that acute ICV infusion[44] or microinjection into the paraventricular nucleus of Na^+-rich aCSF[27] causes sympathetic hyperactivity and hypertension in normotensive rats, and pressor responses are enhanced in salt-sensitive rats compared with salt-resistant rats.[44] Abrams *et al.*[45] hypothesized that when MRs bind ligand, there is a subsequent upregulation of ENaCs, which would increase the membrane permeability to sodium in the brain. This response, in the face of transient increases in sodium levels, would lead to membrane depolarization and an increase in neural activity, driving sympathetic outflow and increasing MAP. It has also been reported that in the paraventricular nucleus, it is possible for an increase in intracellular Na^+ caused by a larger extra-/intracellular gradient to increase intracellular Ca^{2+} through the Na^+/Ca^{2+} channel exchanger, and thereby increase Ang II release.[27] Considering these

observations, it is possible that Na^+-rich aCSF in the RVLM increases sympathetic nerve activity and MAP.

The pressor effect was greater in SHRSPs than in WKY rats, and this difference between the strains might have been related to the different neural responsiveness to Na^+-rich aCSF via ENaCs in the RVLM. This pressor effect was partially blocked by the MR blocker eplerenone in SHRSPs, indicating that the effect of Na^+ might be mediated by MR activation. ICV infusion of the MR blockers, spironolactone[46] or benzamil,[47] prevented Na^+-induced sympathoexcitatory and pressor responses in WKY rats. It has also been reported that ICV infusion of eplerenone attenuated ENaC expression in mice with pressure overload.[30] Taken together, these findings suggest that MRs mediate Na^+ via ENaCs or transporters on the cell surface of neurons in the RVLM.

Study limitations

MRs are largely occupied by the glucocorticoid corticosterone,[48] which is present in a higher concentration than aldosterone in the brain.[41] The enzyme 11β-hydroxysteroid dehydrogenase type 2 (11β-HSD2), which is distributed the brainstem, including the nucleus tractus solitarius,[49] rapidly converts corticosterone to an inactive metabolite. Thus, the coexpression of 11β-HSD2 with MRs may identify brain regions that are particularly sensitive to aldosterone. Although the precise expression of 11β-HSD2 in the RVLM has not yet been determined, we found that aldosterone in the RVLM increased blood pressure, and this pressor response was prevented by the MR blocker eplerenone. Therefore, our findings suggest that aldosterone acts on the MRs in the RVLM. We still cannot exclude the possibility that corticosterone, instead of aldosterone, may act on the MRs in the RVLM. Together with the origin of aldosterone in the RVLM as well as the central nervous system, the study regarding ligand-specifying mechanisms has just begun. In addition, we did not determine whether ENaC activity is involved in the neural responsiveness to Na^+-rich aCSF in the RVLM, because we did not measure ENaC activation in the RVLM. However, it is possible that MRs and ENaCs in the RVLM may be involved in this mechanism.

In conclusion, these findings indicate that MRs in the RVLM contribute to the neural mechanisms of hypertension via sympathetic nerve activity, and that increased activity of MRs may be involved in the elevation of blood pressure in SHRSPs.

CONFLICT OF INTEREST

The authors declare no conflict of interest.

ACKNOWLEDGEMENTS

We express our sincere thanks to Naomi Shirouzu for help with the Western blot analysis. This study was supported by the Grants-in-Aid for Scientific Research from the Japan Society for the Promotion of Science (B19390231, S23220013) and, in part, by the Salt Science Research Foundation (1034).

1 Esler M. The 2009 Carl Ludwig Lecture: Pathophysiology of the human sympathetic nervous system in cardiovascular diseases: the transition from mechanisms to medical management. *J Appl Physiol* 2010; **108**: 227–237.
2 Grassi G. Assessment of sympathetic cardiovascular drive in human hypertension: achievements and perspectives. *Hypertension* 2009; **54**: 690–697.
3 Guyenet PG. The sympathetic control of blood pressure. *Nat Rev Neurosci* 2006; **7**: 335–346.
4 Pitt B, Remme W, Zannad F, Neaton J, Martinez F, Roniker B, Bittman R, Hurley S, Kleiman J, Gatlin M. Eplerenone, a selective aldosterone blocker, in patients with left ventricular dysfunction after myocardial infarction. *N Engl J Med* 2003; **348**: 1309–1321.
5 Yagi S, Akaike M, Aihara K, Iwase T, Yoshida S, Sumitomo-Ueda Y, Ikeda Y, Ishikawa K, Matsumoto T, Sata M. High plasma aldosterone concentration is a novel risk factor of cognitive impairment in patients with hypertension. *Hypertens Res* 2011; **34**: 74–78.
6 Endemann DH, Touyz RM, Iglarz M, Savoia C, Schiffrin EL. Eplerenone prevents salt-induced vascular remodeling and cardiac fibrosis in stroke-prone spontaneously hypertensive rats. *Hypertension* 2004; **43**: 1252–1257.
7 Kimura S, Ito M, Tomita M, Hoyano M, Obata H, Ding L, Chinushi M, Hanawa H, Kodama M, Aizawa Y. Role of mineralocorticoid receptor on atrial structural remodeling and inducibility of atrial fibrillation in hypertensive rats. *Hypertens Res* 2011; **34**: 584–591.
8 Min LJ, Mogi M, Iwanami J, Sakata A, Jing F, Tsukuda K, Ohshima K, Horiuchi M. Angiotensin II and aldosterone-induced neuronal damage in neurons through an astrocyte-dependent mechanism. *Hypertens Res* 2011; **34**: 773–778.
9 Nakamura T, Fukuda M, Kataoka K, Nako H, Tokutomi Y, Dong YF, Yamamoto E, Yasuda O, Ogawa H, Kim-Mitsuyama S. Eplerenone potentiates protective effects of amlodipine against cardiovascular injury in salt-sensitive hypertensive rats. *Hypertens Res* 2011; **34**: 817–824.
10 Takeda Y. Effects of eplerenone, a selective mineralocorticoid receptor antagonist, on clinical and experimental salt-sensitive hypertension. *Hypertens Res* 2009; **32**: 321–324.
11 Schild L. The epithelial sodium channel and the control of sodium balance. *Biochim Biophys Acta* 2010; **1802**: 1159–1165.
12 Geerling JC, Loewy AD. Aldosterone in the brain. *Am J Physiol Renal Physiol* 2009; **297**: F559–F576.
13 Amin MS, Wang HW, Reza E, Whitman SC, Tuana BS, Leenen FH. Distribution of epithelial sodium channels and mineralocorticoid receptors in cardiovascular regulatory centers in rat brain. *Am J Physiol Regul Integr Comp Physiol* 2005; **289**: R1787–R1797.
14 Gomez-Sanchez EP, Gomez-Sanchez CM, Plonczynski M, Gomez-Sanchez CE. Aldosterone synthesis in the brain contributes to Dahl salt-sensitive rat hypertension. *Exp Physiol* 2010; **95**: 120–130.
15 Kumar NN, Goodchild AK, Li Q, Pilowsky PM. An aldosterone-related system in the ventrolateral medulla oblongata of spontaneously hypertensive and Wistar-Kyoto rats. *Clin Exp Pharmacol Physiol* 2006; **33**: 71–75.
16 Comer AM, Gibbons HM, Qi J, Kawai Y, Win J, Lipski J. Detection of mRNA species in bulbospinal neurons isolated from the rostral ventrolateral medulla using single-cell RT-PCR. *Brain Res Brain Res Protoc* 1999; **4**: 367–377.
17 Sved AF, Ito S, Sved JC. Brainstem mechanisms of hypertension: role of the rostral ventrolateral medulla. *Curr Hypertens Rep* 2003; **5**: 262–268.
18 Hirooka Y. Oxidative stress in the cardiovascular center has a pivotal role in the sympathetic activation in hypertension. *Hypertens Res* 2011; **34**: 407–412.
19 Kishi T, Hirooka Y, Kimura Y, Ito K, Shimokawa H, Takeshita A. Increased reactive oxygen species in rostral ventrolateral medulla contribute to neural mechanisms of hypertension in stroke-prone spontaneously hypertensive rats. *Circulation* 2004; **109**: 2357–2362.
20 Hirooka Y, Sagara Y, Kishi T, Sunagawa K. Oxidative stress and central cardiovascular regulation. - Pathogenesis of hypertension and therapeutic aspects -. *Circ J* 2010; **74**: 827–835.
21 Ito S, Komatsu K, Tsukamoto K, Kanmatsuse K, Sved AF. Ventrolateral medulla AT1 receptors support blood pressure in hypertensive rats. *Hypertension* 2002; **40**: 552–559.
22 Kishi T, Hirooka Y, Konno S, Ogawa K, Sunagawa K. Angiotensin II type 1 receptor-activated caspase-3 through ras/mitogen-activated protein kinase/extracellular signal-regulated kinase in the rostral ventrolateral medulla is involved in sympathoexcitation in stroke-prone spontaneously hypertensive rats. *Hypertension* 2010; **55**: 291–297.
23 Yamori Y, Horie R, Handa H, Sato M, Fukase M. Pathogenetic similarity of strokes in stroke-prone spontaneously hypertensive rats and humans. *Stroke* 1976; **7**: 46–53.
24 Zhu DN, Xue LM, Li P. Cardiovascular effects of microinjection of corticoids and antagonists into the rostral ventrolateral medulla in rats. *Blood Press* 1995; **4**: 55–62.
25 Matsukawa R, Hirooka Y, Nishihara M, Ito K, Sunagawa K. Neuregulin-1/ErbB signaling in rostral ventrolateral medulla is involved in blood pressure regulation as an anti-hypertensive system. *J Hypertens* 2011; **29**: 1735–1742.
26 Koga Y, Hirooka Y, Araki S, Nozoe M, Kishi T, Sunagawa K. High salt intake enhances blood pressure increase during development of hypertension via oxidative stress in rostral ventrolateral medulla of spontaneously hypertensive rats. *Hypertens Res* 2008; **31**: 2075–2083.
27 Gabor A, Leenen FH. Mechanisms in the PVN mediating local and central sodium-induced hypertension in Wistar rats. *Am J Physiol Regul Integr Comp Physiol* 2009; **296**: R618–R630.
28 Huang BS, White RA, Jeng AY, Leenen FH. Role of central nervous system aldosterone synthase and mineralocorticoid receptors in salt-induced hypertension in Dahl salt-sensitive rats. *Am J Physiol Regul Integr Comp Physiol* 2009; **296**: R994–R1000.
29 Huang BS, Leenen FH. Blockade of brain mineralocorticoid receptors or Na+ channels prevents sympathetic hyperactivity and improves cardiac function in rats post-MI. *Am J Physiol Heart Circ Physiol* 2005; **288**: H2491–H2497.
30 Ito K, Hirooka Y, Sunagawa K. Blockade of mineralocorticoid receptors improves salt-induced left-ventricular systolic dysfunction through attenuation of enhanced sympathetic drive in mice with pressure overload. *J Hypertens* 2010; **28**: 1449–1458.
31 Wulff P, Vallon V, Huang DY, Volkl H, Yu F, Richter K, Jansen M, Schlunz M, Klingel K, Loffing J, Kauselmann G, Bosl MR, Lang F, Kuhl D. Impaired renal Na(+) retention in the sgk1-knockout mouse. *J Clin Invest* 2002; **110**: 1263–1268.
32 Shibata S, Nagase M, Yoshida S, Kawachi H, Fujita T. Podocyte as the target for aldosterone: roles of oxidative stress and Sgk1. *Hypertension* 2007; **49**: 355–364.

33 Zhou ZH, Bubien JK. Nongenomic regulation of ENaC by aldosterone. *Am J Physiol Cell Physiol* 2001; **281**: C1118–C1130.
34 Gros R, Ding Q, Armstrong S, O'Neil C, Pickering JG, Feldman RD. Rapid effects of aldosterone on clonal human vascular smooth muscle cells. *Am J Physiol Cell Physiol* 2007; **292**: C788–C794.
35 Dampney RAL. Functional organization of central pathways regulating the cardiovascular system. *Physiol Rev* 1994; **74**: 323–364.
36 Zhang ZH, Yu Y, Kang YM, Wei SG, Felder RB. Aldosterone acts centrally to increase brain renin-angiotensin system activity and oxidative stress in normal rats. *Am J Physiol Heart Circ Physiol* 2008; **294**: H1067–H1074.
37 Huang BS, Leenen FH. Mineralocorticoid actions in the brain and hypertension. *Curr Hypertens Rep* 2011; **13**: 214–220.
38 Wang H, Huang BS, Leenen FH. Brain sodium channels and ouabainlike compounds mediate central aldosterone-induced hypertension. *Am J Physiol Heart Circ Physiol* 2003; **285**: H2516–H2523.
39 Huang BS, Leenen FH. Sympathoexcitatory and pressor responses to increased brain sodium and ouabain are mediated via brain II ANG. *Am J Physiol* 1996; **270**: H275–H280.
40 Teruya H, Yamazato M, Muratani H, Sakima A, Takishita S, Terano Y, Fukiyama K. Role of ouabain-like compound in the rostral ventrolateral medulla in rats. *J Clin Invest* 1997; **99**: 2791–2798.
41 Gomez-Sanchez EP, Ahmad N, Romero DG, Gomez-Sanchez CE. Is aldosterone synthesized within the rat brain? *Am J Physiol Endocrinol Metab* 2005; **288**: E342–E346.
42 Yu Y, Wei SG, Zhang ZH, Gomez-Sanchez E, Weiss RM, Felder RB. Does aldosterone upregulate the brain renin-angiotensin system in rats with heart failure? *Hypertension* 2008; **51**: 727–733.
43 Shibata S, Nagase M, Yoshida S, Kawarazaki W, Kurihara H, Tanaka H, Miyoshi J, Takai Y, Fujita T. Modification of mineralocorticoid receptor function by Rac1 GTPase: implication in proteinuric kidney disease. *Nat Med* 2008; **14**: 1370–1376.
44 Huang BS, Wang H, Leenen FH. Enhanced sympathoexcitatory and pressor responses to central Na+ in Dahl salt-sensitive vs. -resistant rats. *Am J Physiol Heart Circ Physiol* 2001; **281**: H1881–H1889.
45 Abrams JM, Osborn JW. A role for benzamil-sensitive proteins of the central nervous system in the pathogenesis of salt-dependent hypertension. *Clin Exp Pharmacol Physiol* 2008; **35**: 687–694.
46 Huang BS, Cheung WJ, Wang H, Tan J, White RA, Leenen FH. Activation of brain renin-angiotensin-aldosterone system by central sodium in Wistar rats. *Am J Physiol Heart Circ Physiol* 2006; **291**: H1109–H1117.
47 Nishimura M, Ohtsuka K, Nanbu A, Takahashi H, Yoshimura M. Benzamil blockade of brain Na+ channels averts Na(+)-induced hypertension in rats. *Am J Physiol* 1998; **274**: R635–R644.
48 de Kloet ER, Van Acker SA, Sibug RM, Oitzl MS, Meijer OC, Rahmouni K, de Jong W. Brain mineralocorticoid receptors and centrally regulated functions. *Kidney Int* 2000; **57**: 1329–1336.
49 Geerling JC, Kawata M, Loewy AD. Aldosterone-sensitive neurons in the rat central nervous system. *J Comp Neurol* 2006; **494**: 515–527.